European Cells and Materials Vol. 43 2022 (pages 202-227) DOI: 10.22203/eCM.v043a15 ISSN 1473-2262

TOWARDS NOVEL MEASUREMENTS OF REMODELLING ACTIVITY IN CORTICAL BONE: IMPLICATIONS FOR OSTEOPOROSIS AND RELATED PHARMACEUTICAL TREATMENTS

L.L. Loundagin and D.M.L. Cooper

Department of Anatomy, Physiology and Pharmacology, University of Saskatchewan, 105 Administration Place, Saskatoon, SK S7N 5A2, Canada

Abstract

Bone remodelling is performed by basic multicellular units (BMUs) that resorb and subsequently form discrete packets of bone tissue. Normally, the resorption and formation phases of BMU activity are tightly coupled spatially and temporally to promote relatively stable bone mass and bone quality. However, dysfunctional remodelling can lead to bone loss and is the underlying cause of osteoporosis. This review surveys how BMU activity is altered in postmenopausal, disuse and glucocorticoid-induced osteoporosis as well as the impact of anabolic and anti-resorptive pharmaceutical treatments. The dysfunctional remodelling observed during disease and following medical intervention bares many testable hypotheses regarding the regulation of BMU activity and may provide novel insights that challenge existing paradigms of remodelling dynamics, particularly the poorly understood BMU coupling mechanisms. Most bone remodelling research has focused on trabecular bone and 2D analyses, as technical challenges limit the direct assessment of BMU activity in cortical bone. Recent advances in imaging technology present an opportunity to investigate cortical bone remodelling *in vivo*. This review discusses innovative experimental methods, such as 3D and 4D (*i.e.* time-lapsed) evaluation of BMU morphology and trajectory, that may be leveraged to improve the understanding of the spatio-temporal coordination of BMUs in cortical bone.

Keywords: Basic multicellular unit, cortical bone, bone remodelling, *in vivo* micro-computed tomography, time-lapsed imaging, *in silico* models.

***Address for correspondence**: Lindsay L. Loundagin, Department of Anatomy, Physiology and Pharamcology, University of Saskatchewan, 107 Wiggins Road, Saskatoon, SK S7N 5E5, Canada.
Email: ll.loundagin@usask.ca

List of Abbreviations

ATP	adenosine 5′-triphosphate
BMU	basic multicellular unit
DMP-1	dentine matrix acidic phosphoprotein 1
DKK1	Dickkopf WNT signalling pathway inhibitor 1
FE	finite element
FGF23	fibroblast growth factor 23
HR-pQCT	high resolution-peripheral computed tomography
IL	interleukin
MEPE	matrix extracellular phosphoglycoprotein
OPG	osteoprotegerin
OVX	ovariectomised
PTH	parathyroid hormone
RANK	receptor activator of nuclear factor κB
RANKL	RANK ligand
SR	synchrotron radiation
TGF-β	transforming growth factor beta
TNF	tumour necrosis factor
μCT	micro-computed tomography

Introduction

Bone remodelling provides a mechanism to maintain, repair and replace bone in the adult skeleton. This continuous turnover is achieved by a temporary collection of cells known as a BMU (Frost, 1969). In cortical bone, BMUs create a tunnel-like remodelling space in which a cutting cone formed by osteoclasts erodes the bone matrix and is subsequently filled by osteoblasts forming new bone in the closing cone (Fig. 1**b**). The finished product is a secondary osteon (*i.e.* Haversian system), whose diameter and wall thickness are indicative of the amount of bone resorbed and formed, respectively, by a single BMU (Fig. 1**a**). Although the mechanisms that govern the reversal of bone resorption to bone formation are still not well understood, these two phases are believed to be strongly coupled both spatially and temporally (Andersen *et al.*, 2013; Parfitt, 1982). A remodelling event is considered to be balanced when the amount of bone resorbed and formed is equal such that the overall porosity and bone mineral density remain relatively constant. Excessive or dysfunctional (*i.e.* imbalanced or uncoupled; Fig. 1**c**) BMU activity can drastically increase the intracortical porosity and is a hallmark of common bone diseases such as osteoporosis (Kenkre and Bassett, 2018).

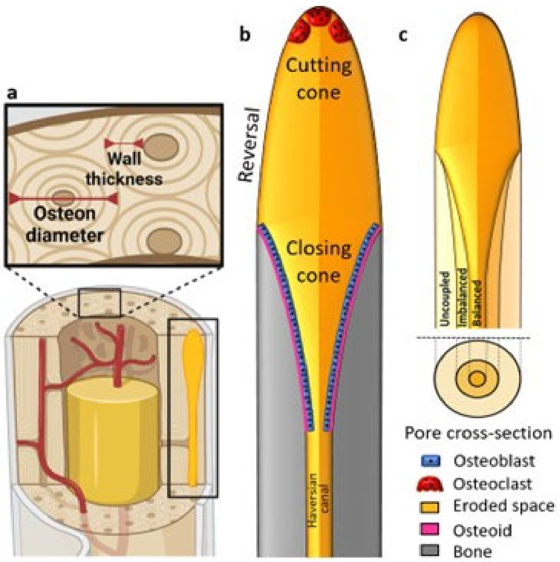

Fig. 1. Schematic of a BMU in cortical bone. (**a**) Sectioned view of cortical bone illustrating the osteonal structure resulting from remodelling by BMUs and the common measurements of osteon morphology – osteon diameter and wall thickness – indicative of BMU activity. (**b**) Schematic of a BMU and (**c**) its relationship to osteon structure in uncoupled, imbalanced and balanced conditions.

Increased cortical porosity explains up to 76 % of the variance in bone strength (McCladen *et al.*, 1993) and is a primary risk factor for fragility fractures (Bjørnerem, 2016; Pisani *et al.*, 2016; Ramchand and Seeman, 2018; Zebaze *et al.*, 2010). Pores decrease bone strength by both reducing the load-bearing capacity and by acting as stress concentrations (Currey, 1962; Hernandez *et al.*, 2006; Wachter *et al.*, 2002). Pores diminish the total amount of material available to withstand a given load and, therefore, decrease the bone's load-carrying capacity. Additionally, pores are stress concentrators in the bone matrix that locally elevate the stress, making surrounding regions more susceptible to developing and accumulating microcracks (Loundagin *et al.*, 2020; Nicolella *et al.*, 2006). Cavities of various sizes and functions contribute to cortical porosity, most notably, osteocyte lacunae and vascular canals (Cooper *et al.*, 2016). However, given that BMU activity dictates the morphology of the canal network and is the focus of the present review, cortical porosity herein refers to the latter.

The more abundant and larger canals associated with age-related and pathological bone loss (Fig. 2) are primarily driven by a high rate of remodelling and a negative balance in BMU activity (Andreasen *et al.*, 2018). Even when balanced, faster bone resorption relative to a slower rate of formation may create a transient, albeit potentially reversible, increase in

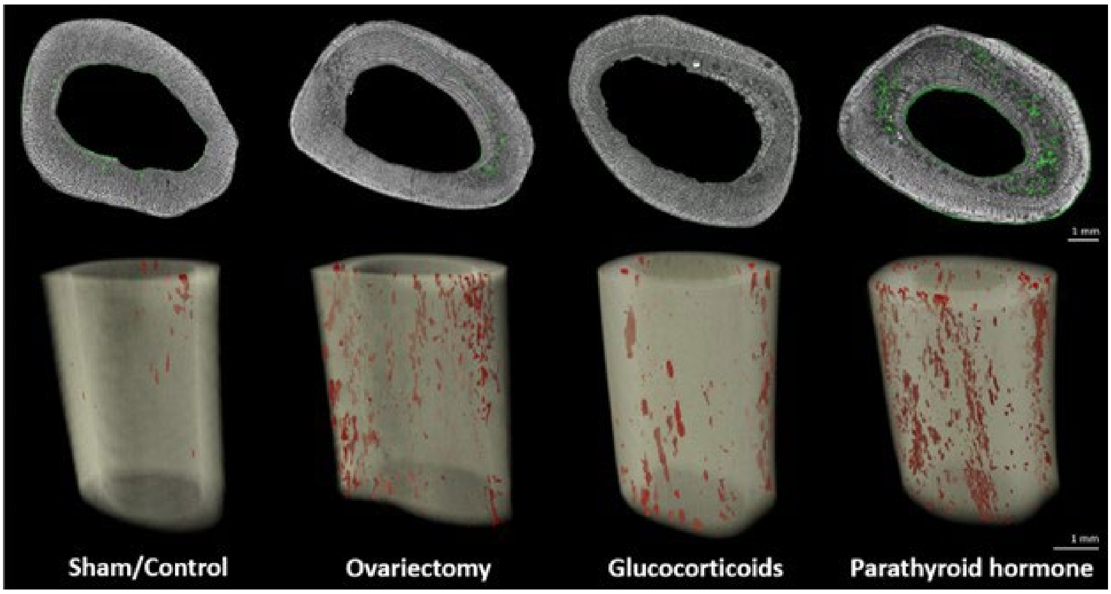

Fig. 2. Intracortical remodelling in rabbit tibiae from various treatment groups. (Top) Representative transverse cross-sections of rabbit tibiae from various treatment groups imaged using differential interference contrast and fluorescent confocal microscopy. Active bone formation is labelled with calcein (green fluorescent signal). Note: calcein labels are absent from the glucocorticoid-treated rabbits due to deficient bone formation. (Bottom) 3D μCT images (nominal resolution = 10 μm) of the corresponding specimen illustrating the intracortical porosity related to remodelling cavities (red). Data and images courtesy of Dr Kim Harrison (Harrison *et al.*, 2020a).

porosity (Martin, 1991). Emerging evidence also suggests that slower resorption may delay or even completely inhibit the onset of bone formation (*i.e.* uncoupling) (Lassen *et al.*, 2017). Both scenarios illustrate the delicate and intertwined nature of bone resorption and formation and how their spatio-temporal relationship determines the success of a given remodelling event. Additionally, prolonged intracortical remodelling increases the density of pores, which may merge, creating fewer but markedly larger pores (Andreasen *et al.*, 2018; Bell *et al.*, 2001). Therefore, the aspects of BMU activity that dictate intracortical porosity are 1) the activation frequency (*i.e.* birth rate) of BMUs; 2) the relative volumes of bone resorbed and formed; 3) the spatio-temporal relationship between bone resorption and formation; 4) the spatial distribution and trajectory of BMUs (*i.e.* coalescence of active BMUs and/or existing canals).

These four parameters are believed to be altered with age and disease and, as such, are the target of many therapeutic strategies attempting to mitigate the deleterious effects of dysfunctional remodelling (Kenkre and Bassett, 2018). Bone loss in both primary (*e.g.* senile or postmenopausal) and secondary (*e.g.* disease- or drug-induced) osteoporosis is a consequence of accelerated bone turnover and a net increase in bone resorption. Pharmaceutical treatment of osteoporosis is typically categorised into 2 approaches, anabolic and anti-resorptive therapies. PTH and romosozumab are anabolic therapies that increase bone mass by stimulating bone formation (Aslan *et al.*, 2012). More commonly used anti-resorptive treatments, such as bisphosphonates and denosumab, reduce bone resorption by limiting osteoclastic activity (Baron *et al.*, 2011). Despite the prevalence of osteoporosis and moderate success of pharmaceutical treatments in preventing fragility fractures (Sozen *et al.*, 2017; Vandenbroucke *et al.*, 2017), the intricacies of pathophysiological bone remodelling and the role of pharmaceutical interventions in restoring remodelling dynamics at the BMU-level are largely unknown.

This knowledge gap is especially evident for cortical bone, as most bone remodelling research has focused on trabecular bone loss. This is exacerbated by the fact that the spatio-temporal coordination of BMUs remains a challenge to observe directly *in vivo*. Current understanding of 3D BMU morphology in cortical bone comes from a limited number of studies utilising serial sectioning (Fig. 3**a**); however, these data are inherently static and provide merely a snapshot of BMU activity. Knowledge of dynamic (*i.e.* time-lapsed) BMU activity is largely derived from dynamic histomorphometry studies in which fluorochrome labelling of newly calcified bone at multiple timepoints allows calculation of mineral apposition and bone formation rates (Fig. 3**b**). Importantly, dynamic histomorphometry only provides a direct assessment of the formative phase and aspects of the resorptive phase can only be inferred indirectly. Furthermore, the detection of fluorochrome labels can be highly variable depending on the status of the closing cone at the time of label administration or biopsy (Buenzli *et al.*, 2014) and possibly undetectable if bone formation is impaired or uncoupled, as is the case of glucocorticoid-induced osteoporosis (Dalle Carbonare *et al.*, 2005; Jensen *et al.*, 2015).

Identifying how and why BMU activity varies is crucial to better understand the physiological and pathophysiological process of bone remodelling as well as an essential component in managing or preventing associated bone loss. The ability of current methods to directly assess BMU activity is limited.

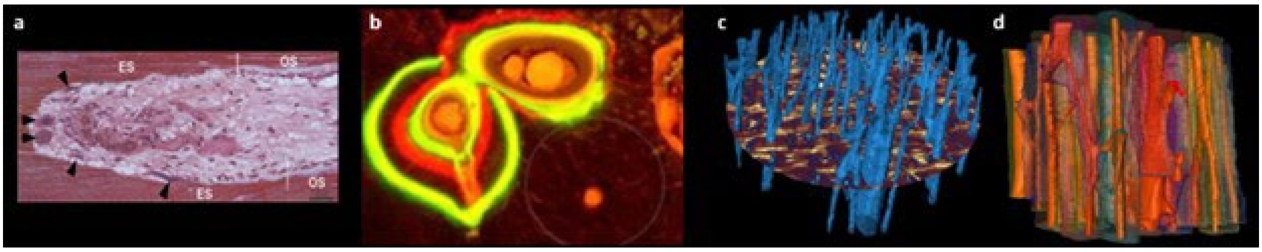

Fig. 3. The variety of techniques used to investigate bone remodelling. (**a**) Bone histomorphometry can detect the presence and spatial relationship of cells as well as characterise activity-specific surfaces. This histological longitudinal section of a BMU in the fibula of a 65-year-old man stained with Masson's trichrome illustrates the presence of osteoclasts (black arrowheads) distributed along the eroded surface (ES) of the cutting cone, up to the point where bone formation begins on the osteoid surface (OS). (**b**) Dynamic histomorphometry uses fluorochrome labelling of newly calcified bone to quantify changes in bone formation as a function of time. Calcein (green) and alizarin red labels administered every 14 d demonstrate the active bone formation occurring in the canine tibia under loading conditions. (**c**) μCT and (**d**) SR μCT imaging are non-destructive techniques that allow a 3D perspective on intracortical porosity, which is essential in understanding the activity of a BMU over its lifespan. (**c**) The fusion of μCT and 2D histology illustrates the complexity of the microarchitecture extending beyond what is seen in a 2D section, and SR μCT has the capability to capture minute details such as the cement lines (*i.e.* osteon borders) surrounding the (**d**) vascular canals. All figures were used with permission from the copyright owner and reprinted from the following publications: (**a**) Lassen *et al.*, 2017; (**b**) Hui *et al.*, 2016; (**c**) Hennig *et al.*, 2015; (**d**) Maggiano *et al.*, 2016.

At best, the dynamic nature of only the formative phase is quantifiable and the coordination of the resorptive and reversal phases remains elusive. The present review examines how specific parameters of BMU activity may be altered in osteoporosis (postmenopausal, disuse and glucocorticoid-induced) and with pharmaceutical therapies, including anabolic (PTH and romosozumab) and anti-resorptive treatments (bisphosphonates and denosumab). This is followed by a discussion on existing and future experimental methods that may be leveraged to improve the understanding of the spatio-temporal coordination of BMUs.

Altered BMU activity in disease and with drug

Changes in remodelling dynamics at the BMU-level are typically evaluated by the amount and rate of bone resorption and formation. Resorptive activity is quantified by erosion depth, erosion period and abundance as well as the length of eroded surfaces. Erosion surfaces are typically defined as scalloped surfaces that may be active (osteoclasts are present) or inactive (without osteoclasts). The erosion period represents the average time taken to resorb the osteon cavity but is an indirect measurement based on labels of bone formation. In trabecular bone, erosion depth is the depth of the cavity relative to an adjacent bone surface and indicates the amount of bone resorbed by a single BMU, similar to the measurement of osteon diameter used in cortical bone (Fig. 1**a**). Bone formation in both cortical and trabecular bone is assessed by mineral apposition rate, wall thickness as well as length and number of mineralising surfaces. Mineral apposition rate represents the linear rate of new bone deposition, measured as the distance between two consecutive fluorochrome labels divided by the labelling period. Mineralising surface is based on the extent of the labelled surface to describe the amount of mineralisation at a particular time. The following section reviews the underlying processes that alter these variables, how they contribute to bone loss in postmenopausal, disuse and glucocorticoid-induced osteoporosis, and discusses several drug treatments that manipulate parameters of BMU activity to restore remodelling dynamics.

Osteoporosis

Postmenopausal osteoporosis

Postmenopausal osteoporosis, a primary form of the disease, is a common bone disorder caused by oestrogen deficiency. Under normal conditions, oestrogen has a protective effect on bone, limiting the differentiation and activity of osteoclasts. Oestrogen suppresses TNF and IL-1, cytokines known to enhance osteoclast activity (Charatcharoenwitthaya *et al.*, 2007; Jilka, 1998; Pacifici *et al.*, 1991), as well as IL-6, which stimulates osteoclastogenesis (Jilka *et al.*, 1992). Osteoclast life span is indirectly controlled through oestrogen-mediated regulation of TGF-β (Hughes *et al.*, 1996) and promotes apoptosis of mature osteoclasts directly *via* FAS ligand/FAS signalling (Krum *et al.*, 2008; Wang *et al.*, 2015). Oestrogen also stimulates OPG expression (Bord *et al.*, 2004; Saika and Matsumoto, 2001), disrupting the RANK/RANKL pathway, which largely controls osteoclast formation in osteoclast precursors as well as the activation and survival of mature osteoclasts (Boyce and Xing, 2007; Lacey *et al.*, 1998; Shevde *et al.*, 2000). With the decline in oestrogen associated with menopause, osteoclasts are more abundant, active and survive longer (Nakamura *et al.*, 2007; Weitzmann and Pacifici, 2006), all of which may contribute to increased resorption, porosity and bone fragility.

Although these changes in osteoclast fate, function and survival have been observed at the cellular level, the implication of larger resorption cavities is not directly reflected in histomorphometric analyses of osteoporotic bone. Indeed, bone biopsies from the iliac crest of osteoporotic women exhibit more osteoclasts and a 45 % increase in BMU activation frequency than that of healthy postmenopausal women, but erosion depth is comparable between the two groups (Cohen-Solal *et al.*, 1991; Eriksen *et al.*, 1990). 3D evaluation of trabecular bone loss in OVX rat and mouse models also present conflicting evidence. OVX mice demonstrated fewer resorption sites but larger erosion surfaces per site (Lambers *et al.*, 2012). On the other hand, the increased bone resorption in OVX rats was due to an increased frequency in resorption cavities with no difference in the total volume resorbed per cavity (Slyfield *et al.*, 2012). The latter would suggest that oestrogen deficiency primarily affects bone remodelling by increasing the activation frequency but not the function of active BMUs and challenges the belief that increased osteoclast number and osteoclast surface observed in osteoporotic bone must yield increased resorption at the BMU-level (Arlot *et al.*, 1990). While it is true that resorption is increased globally in osteoporosis, more data is needed to understand the importance and respective contributions of remodelling frequency and resorption volume to total bone loss.

Dynamic parameters of BMU activity in human bone are primarily reported for the trabecular and endocortical envelopes and remain largely unknown for intracortical bone. Static measurements of osteon morphology provide some indication of remodelling activity in cortical bone. For example, the number of osteons observed in the femoral cortex of osteoporotic females was larger than that in young, healthy females (Zimmermann *et al.*, 2016), while osteon diameter in osteoporotic bone was smaller compared to young healthy bone (Bernhard *et al.*, 2013). Similar to what has been reported for trabecular and endocortical bone, activation frequency in cortical bone is increased in postmenopausal osteoporosis; however, the resorption volume and period in cortical bone may actually be lower. Interestingly, resorption per BMU is reduced in postmenopausal osteoporotic women (Bernhard *et al.*, 2013) even though the number, activity and lifespan of osteoclasts are thought to be increased (Nakamura *et al.*, 2007).

It is largely agreed that bone formation is impaired in osteoporosis and contributes to the imbalance between resorption and formation at the BMU level, in favour of resorption. Mean wall thickness, an indication of the amount of bone formed per remodelling event, is lower in both osteoporotic trabecular (Cohen-Solal *et al.*, 1991; Darby and Meunier, 1981; Eriksen *et al.*, 1990; Kimmel *et al.*, 1990; Parfitt *et al.*, 1995) and cortical bone (Bernhard *et al.*, 2013). Varying findings have been reported for mineral apposition rate, describing that of postmenopausal osteoporosis as either decreased (Carasco *et al.*, 1989; Eriksen *et al.*, 1990; Parfitt *et al.*, 1995) or unchanged (Arlot *et al.*, 1990; Kimmel *et al.*, 1990) compared to non-osteoporotic postmenopausal controls. Diminished bone formation may indicate a disruption in BMU coordination, hindering the reversal of bone resorption to formation due to impaired recruitment or function of osteoblasts, or both. Finally, elevated cortical porosity may be compounded by the coalescence of active BMUs or remodelling of existing canals. This phenomenon plays a role in the increasing porosity associated with age (Andreasen *et al.*, 2018) and has been suggested to contribute to the presence of fewer but larger mineralising surfaces in OVX rats (Slyfield *et al.*, 2012). Taken together, histological evidence indicates that the increased intracortical porosity in osteoporosis is a result of higher activation frequency, insufficient bone formation and merging of remodelling spaces rather than an excessive amount of bone resorbed per remodelling event.

Glucocorticoid-induced osteoporosis

Glucocorticoids are a group of immunomodulating drugs commonly used to treat autoimmune disorders and inflammatory conditions; however, glucocorticoid treatment is associated with rapid bone loss and fragility fractures (Van Staa *et al.*, 2002) and is the leading cause of secondary osteoporosis (Adami and Saag, 2019; Whittier and Saag, 2016). Pharmacological doses of glucocorticoids induce osteoporosis by altering bone remodelling, affecting cells from both the osteoblast and osteoclast lineages. Yet, the most notable characteristic of glucocorticoid-induced osteoporosis is deficient bone formation and is primarily due to a reduced number of osteoblastic cells and impaired osteoblast function (Canalis *et al.*, 2007). Glucocorticoids inhibit the differentiation of osteoblasts (Ohnaka *et al.*, 2004; Pereira *et al.*, 2002) and promote apoptosis of osteoblasts and osteocytes (Weinstein *et al.*, 1998). The quality of the bone matrix is also diminished as glucocorticoids enhance the expression of mineralisation inhibitors, DMP-1 and Phex (Yao *et al.*, 2008), and suppresses osteocalcin and type I collagen (Canalis, 1983; Godschalk and Downs, 1988; Hernández *et al.*, 2004; Peretz *et al.*, 1989). Osteoclast formation and activity are enhanced with glucocorticoids (Hofbauer *et al.*, 1999; Sivagurunathan *et al.*, 2005) and they may also affect the life span of osteoclasts, although opposing results have been reported (Jia *et al.*, 2006; Kim *et al.*, 2006; Sivagurunathan *et al.*, 2005).

Given the significantly reduced bone formation with glucocorticoids, double-fluorochrome labels of mineralising surfaces are often absent (Fig. 2) and using dynamic histomorphometry to assess aspects of BMU activity, particularly mineral apposition rate and activation frequency, is futile (Harrison *et al.*, 2020a; Schorlemmer *et al.*, 2005). When detectable, the number and length of mineralising surfaces (Carbonare *et al.*, 2001; Schorlemmer *et al.*, 2005), wall thickness (Carbonare *et al.*, 2001; Dempster *et al.*, 1983; Vedi *et al.*, 2005) and mineral apposition rate (Bressot *et al.*, 1979; Dempster *et al.*, 1983; Vedi *et al.*, 2005) are decreased with glucocorticoid treatment compared to untreated controls. The influence of glucocorticoids on the activation frequency and resorptive activity of BMUs is less clear. The rapid rate of bone loss within the first 3-6 months of glucocorticoid treatment has led some to suggest that BMU activation frequency and resorption is elevated shortly after treatment initiation and followed by a more gradual decline in bone mass with continued treatment, during which activation frequency and resorption return to normal but formation is still impaired. This transient behaviour is supported by some (Dovio *et al.*, 2004; Haris *et al.*, 2012; Yao *et al.*, 2008), but not all (Ebeling *et al.*, 1998; Prummel *et al.*, 1991; Sasaki *et al.*, 2002), studies utilising biochemical markers of bone turnover and the histological evidence of changes in activation frequency and resorption are limited because these parameters are typically derived from labels of bone formation. Two studies report decreased activation frequency in cortical bone after long-term treatment with glucocorticoids in humans (Vedi *et al.*, 2005) and OVX sheep (Schorlemmer *et al.*, 2005). To circumvent the reliance on formative activity, Harrison *et al.* (2020a) defined "active remodelling centres" as a measure of remodelling activity in rabbits that included the sum of single-labelled osteons, double-labelled osteons and resorption cavities normalised to cortical area. In contrast to reports in human and OVX sheep (Schorlemmer *et al.*, 2005; Vedi *et al.*, 2005), they found that active remodelling centres in glucocorticoid-treated rabbits were 3-fold larger than in sham controls (Fig. 2) (Harrison *et al.*, 2020a). Increased erosion surface, more abundant osteoclasts and larger canal diameters imply that resorption may be enhanced (Bressot *et al.*, 1979; Carbonare *et al.*, 2001; Harrison *et al.*, 2020a), yet direct measurement of resorption capacity at the BMU-level (*e.g.* erosion depth or osteon diameter) has not been reported. Whether resorptive activity is maintained or elevated, it is apparent that bone resorption is ongoing with glucocorticoids treatment without subsequent formation, indicating BMU uncoupling. Jensen *et al.* (2015) have demonstrated that the absence of bone formation in glucocorticoid treatment is associated with arrested reversal surfaces in which resorption has finished with no evidence of ongoing or future bone formation. In fact, arrested reversal surfaces were 5-times higher in glucocorticoid-treated patients compared to controls (Jensen *et al.*, 2015). This is suggestive of BMU uncoupling and may be the underlying cause of bone loss in glucocorticoid-induced osteoporosis (Andreasen *et al.*, 2015). It is important to note that the overall bone loss due to excess glucocorticoids is not the only contributor to reduced bone strength. Glucocorticoid treatment also compromises the quality of the bone matrix on the nanoscale and microscale, including decreased mineralisation as well as altered collagen content and organisation, which may negatively affect bone strength at the organ (*i.e.* whole-bone) level (Saito *et al.*, 2011; Xi *et al.*, 2020).

Disuse osteoporosis

Bone remodelling is also regulated by the mechanical environment. The link between bone remodelling and mechanical loading was formally introduced in the "mechanostat theory" (Frost, 1987). Frost proposed that loading bone above a given strain would lead to bone formation through the modelling process, while underloading would enable bone resorption through increased remodelling. The latter may result in significant bone loss that is clinically referred to as disuse osteoporosis. Clinical examples of disuse osteoporosis include immobilisation during long-term bed rest or after fracture, spinal cord injury, paralysis and other neuromuscular or neurological disorders (Giangregorio and McCartney, 2006; Iolascon *et al.*, 2019; Rolvien and Amling, 2021; Zerwekh *et al.*, 1998). Reduced skeletal loads in microgravity during spaceflight may also lead to significant bone loss consistent with disuse osteoporosis (Gabel *et al.*, 2021; Stavnichuk *et al.*, 2020).

Mechanosensitive osteocytes are key players in the pathogenesis of disuse osteoporosis. Embedded in the bone matrix, osteocytes sense and translate changes in the mechanical environment to biochemical signals that regulate gene expression (Santos *et al.*, 2009). It is through this mechanotransduction that osteocytes orchestrate bone remodelling in response to increased mechanical loading. Mechanical stimulus promotes osteocyte survival (Bakker *et al.*, 2004; Plotkin *et al.*, 2005) and removal of such a stimulus enhances osteocyte apoptosis (Gerbaix *et al.*, 2017; Mann *et al.*, 2006; Rolvien *et al.*, 2020), triggering bone resorption (Aguirre *et al.*, 2006; Cabahug-Zuckerman *et al.*, 2016). Nitric oxide is a regulatory molecule produced by osteocytes that inhibits bone resorption by enhancing OPG and reducing RANKL expression, thereby limiting osteoclastogenesis (Fan *et al.*, 2004). Simulated microgravity has been associated with decreased nitric oxide production in MLO-Y4 osteocyte-like cells *in vitro* (Xu *et al.*, 2012) and may potentiate bone resorption (Nabavi *et al.*, 2011; Ralston *et al.*, 1995). Unloading also increases osteocyte expression of RANKL and results in increased number and activity of osteoclasts (Cabahug-Zuckerman *et al.*, 2016; Maïmoun *et al.*, 2005; Tamma *et al.*, 2009; Xiong *et al.*, 2011). Sclerostin and DKK1 are antagonists of the WNT signalling pathway that inhibit osteoblast function. Both sclerostin and DKK1 are increased after unloading (Gaudio *et al.*, 2010; Gifre *et al.*, 2015; Lin *et al.*, 2009; Spatz *et al.*, 2012) and may be responsible for the reduced number of osteoblasts and impaired bone formation (Li *et al.*, 2006; Lin *et al.*, 2009). Additional signalling molecules such as ATP and prostaglandins are upregulated following increases in mechanical stimuli and contribute to improved osteoblast differentiation, proliferation and function (Bonewald, 2011; Brunet *et al.*, 2004; Genetos *et al.*, 2004; Liu *et al.*, 2017); however, little evidence is available to assess their role in the case of unloading. Disuse may also lead to alterations in bone mineralisation. Reduced levels of serum osteocalcin have been reported in rats after 7 d of spaceflight (Patterson-Buckendahl *et al.*, 1987) and a more homogenous mineral distribution in immobilised elderly females (Rolvien *et al.*, 2020). Changes in mineralisation may be related to mineralisation regulators such as FGF23, MEPE and DMP-1, which are known to be produced by osteocytes in a mechanically sensitive manner (Harris *et al.*, 2007; Nepal *et al.*, 2021; Yang *et al.*, 2005).

Many studies report marked bone loss and elevated biomarkers of bone resorption following various models of unloading (Rolvien and Amling, 2021; Stavnichuk *et al.*, 2020); however, far fewer have reported specific changes in resorptive activity. Nonetheless, these studies support the notion of increased resorption following unloading, with an increased number of remodelling spaces (Kazakia *et al.*, 2014; Li *et al.*, 2004), larger osteons (Li *et al.*, 2004; Young *et al.*, 1986), more abundant osteoclasts (Ishijima *et al.*, 2001; Kondo *et al.*, 2005; Weinreb *et al.*, 1989) as well as increased erosion and osteoclast surfaces (Ishijima *et al.*, 2001; Kondo *et al.*, 2005; Li *et al.*, 1990; Li and Jee, 1991; Weinreb *et al.*, 1989; Zerwekh *et al.*, 1998). Alterations in bone formation due to unloading has been documented more extensively. Mineral apposition rate and mineralising surface are reduced following hind-limb unloading, denervation or tail suspension in rats (Drissi *et al.*, 1999; Ishijima *et al.*, 2001; Kondo *et al.*, 2005; Li *et al.*, 1990; Li and Jee, 1991; Turner and Bell, 1986), immobilisation or spaceflight in monkeys (Schock *et al.*, 1975; Young *et al.*, 1986; Zerath *et al.*, 1996) and immobilisation of the equine metacarpophalangeal joint (van Harreveld *et al.*, 2002). Interestingly, Young *et al.* (1986) described the surfaces of large resorption cavities of immobilised monkeys as smooth surfaces lined with mononucleated cells. Given the missing tetracycline labels of bone formation but the presence of mononucleated cells on the erosion surface, the authors hypothesised that osteoblast recruitment may not be compromised but the specific cell function inhibited, resulting in a prolonged reversal phase. The intracortical microarchitecture in long bones seems to mirror the principal stress directions, suggesting that during remodelling a BMU's trajectory through the bone matrix may be guided by mechanical stimuli (Heřt *et al.*, 1994; van Oers *et al.*, 2008a; Petrtýl *et al.*, 1996). Britz *et al.* (2012) demonstrated that the removal of mechanical loading in immobilised rats results in more disorganised canal orientations compared to controls. However, this has not been studied in larger-animal models that exhibit more typical rates of secondary remodelling.

Anabolic treatments

PTH therapy

PTH is a major endocrine regulator of extracellular phosphate and calcium levels. When blood serum calcium levels are low, the parathyroid glands secret PTH, which activates bone remodelling to release calcium stored in the bone matrix. In primary hyperparathyroidism, circulating levels of PTH are constantly elevated, leading to increased bone resorption and marked bone loss (Rubin *et al.*, 2008; Vu *et al.*, 2013). On the other hand, intermittent low-dose administration of PTH (*e.g.* teriparatide) has an anabolic effect, resulting in net bone formation (Hock and Gera, 1992; Locklin *et al.*, 2003) and is, therefore, an effective treatment for severe osteoporosis.

The anabolic effects of intermittent PTH are largely attributed to increased osteoblast abundance and life span. PTH amplifies the number of pre-osteoblasts present in the bone marrow by promoting the commitment of mesenchymal stem cells to the osteoblast lineage (Fan *et al.*, 2017) and increasing the proliferation and differentiation of osteoblasts (Balani *et al.*, 2017). Intermittent PTH augments osteoblast activity and survival by supporting osteoblast maturation and attenuating osteoblast apoptosis (Jilka *et al.*, 1999). Cytokines released from the bone matrix during bone resorption are also essential for the anabolic effects of PTH (Tang *et al.*, 2009). In fact, without resorptive activity, the anabolic capacity of PTH may be limited (Delmas *et al.*, 1995; Wu *et al.*, 2010) and this highlights the importance of coupling in remodelling-based bone formation.

The mechanisms of action and effects of PTH vary among different bone compartments (*i.e.* trabecular, endosteal, periosteal and intracortical envelopes) and may explain some of the differences observed with PTH treatment. For instance, net bone formation is increased on trabecular, endosteal and periosteal surfaces (Jiang *et al.*, 2003; Lindsay *et al.*, 2007; Yamamoto *et al.*, 2016), whereas intermittent PTH significantly increases intracortical porosity (Hansen *et al.*, 2013; Jiang *et al.*, 2003; MacDonald *et al.*, 2011; Yamane *et al.*, 2017). This can mainly be attributed to increased activation frequency (Fig. 2), as observed in rabbits (Harrison *et al.*, 2020a; Hirano *et al.*, 1999), canines (Boyce *et al.*, 1996), monkeys (Burr *et al.*, 2001; Sato *et al.*, 2004) and humans (Ma *et al.*, 2014). The effect of PTH on the resorption capacity of individual BMUs is largely unknown for cortical bone and conflicting data in endocortical bone describe resorption parameters as either increased (Boyce *et al.*, 1996; Hirano *et al.*, 1999), unchanged (Dempster *et al.*, 2016b; Jiang *et al.*, 2003) or decreased (Lindsay *et al.*, 2007). Consistent with the expected increase in osteoblastic activity, PTH has been shown to augment aspects of intracortical bone formation, including increased mineralising surface and mineral apposition rate (Dempster *et al.*, 2016a; Hirano *et al.*, 1999; Ma *et al.*, 2014).

Romosozumab

Romosozumab is an anti-sclerostin antibody recently approved in the United States and Canada as an anabolic treatment for osteoporosis (Web ref. 1; Web ref. 2). Sclerostin, a protein secreted by osteocytes, inhibits the WNT signalling pathway, which stimulates osteoblast differentiation, proliferation and survival. Romosozumab binds to sclerostin to prevent this inhibitory effect and the WNT signalling pathway is activated, in turn increasing bone formation. Clinical trials in postmenopausal women have continually demonstrated that 3-12 months of romosozumab treatment increases BMD at the spine, hip and femoral neck (Cosman *et al.*, 2016; McClung *et al.*, 2014; Padhi *et al.*, 2011). The marked improvements in bone mass may largely be attributed to the increases in modelling-based bone formation (*i.e.* formation on the endocortical and periosteal surface independent of prior resorption) rather than changes in remodelling activity. However, this phase of enhanced modelling-based formation attenuates over time and bone mass may continue to increase due to a net positive balance at remodelling sites (Boyce *et al.*, 2017; Ominsky *et al.*, 2017).

OVX cynomolgus monkeys treated with romosozumab demonstrated an increased mineral apposition rate and proportion of mineralising surfaces on trabecular, periosteal and endocortical surfaces after 3 and 6 months of treatment compared to controls but no significant difference in wall thickness at remodelling sites in trabecular bone. This trend was reversed after 12 months in OVX-treated monkeys, having an increased wall thickness but a similar proportion of mineralising surfaces and mineral apposition rate to that of the OVX-placebo group (Ominsky *et al.*, 2017). Intracortical remodelling was transiently increased, as evidenced by a higher activation frequency, but this did not induce significant changes in cortical porosity despite negligible differences in any measures of bone formation in cortical bone (Ominsky *et al.*, 2017). The recent study by Chavassieux *et al.* (2019a) provides the only histological evidence of romosozumab's effect on human bone, reporting the microstructural indices in all four bone compartments from iliac crest biopsies of postmenopausal osteoporotic women after 2 and 12 months of treatment. In general, their findings agree with what has been observed in primates: mineralising surfaces were increased on trabecular and endocortical surfaces after 2 months of treatment, but these values returned to or below control levels by 12 months, while wall thickness in trabecular bone remained elevated after 12 months of drug treatment. In contrast, the authors did not find an increase in mineral apposition rate within any of the bone compartments at either the 2- or 12-month timepoint. Activation frequency was only measured in trabecular bone but, similar to the trend observed in cortical bone in primates, demonstrated a transient increase, being nearly double that of the placebo group at 2 months and 5 times lower at 12 months (Chavassieux *et al.*, 2019a).

Interestingly, gains in BMD with romosozumab treatment are greater than those in patients treated with PTH (Genant *et al.*, 2017; Langdahl *et al.*, 2017; McClung *et al.*, 2014). This may be because romosozumab is not solely an anabolic agent, but rather has a dual action, increasing bone formation and reducing bone resorption. Sclerostin also promotes increased expression of RANKL by osteocytes. RANKL plays a major role in the formation and function of osteoclasts (Wijenayaka *et al.*, 2011). Therefore, in the presence of romosozumab, reduced RANKL leads to fewer osteoclasts and less resorption (Boyce *et al.*, 2017; Chavassieux *et al.*, 2019a; Kostenuik *et al.*, 2009; Li *et al.*, 2009). In both primates and humans, romosozumab treatment is associated with reduced erosion surfaces and osteoclast number in the trabecular and endocortical compartments (Boyce *et al.*, 2017; Chavassieux *et al.*, 2019a). This diminished resorptive activity is apparent in the early stages of treatment and sustained until the final timepoint. Erosion depth is also lower in romosozumab-treated primates (Boyce *et al.*, 2017), although this has yet to be reported in humans. It is interesting to note that intracortical and trabecular remodelling is increased despite the inhibition of osteoclasts and has led some to hypothesise that this may be a mechanism to support the mineral demands of the enhanced bone formation occurring during the early stages of treatment (Ominsky *et al.*, 2017).

While PTH and romosozumab are both anabolic treatments that cause a net gain in bone mass, the processes by which bone formation is augmented differ. PTH treatment increases both resorption and formation activity in the BMU remodelling process, while romosozumab primarily increases modelling-based bone formation, decreases bone resorption and eventually reduces bone turnover. The combined effects of romosozumab on BMU activity — reducing erosion depth and increasing wall thickness — would result in a net positive balance in individual remodelling events and contribute to increasing BMD; however, more work is needed to determine the role of romosozumab in remodelling dynamics, particularly in human cortical bone.

Anti-resorptive drugs

Systemic and focal bone loss, such as in osteoporosis or rheumatoid arthritis, is often treated with anti-resorptive drugs that target osteoclasts to ultimately reduce the magnitude of bone resorption. Anti-resorptive drugs may decrease bone resorption by 1) limiting the differentiation of osteoclastic precursors into mature resorbing osteoclasts, 2) reducing the activity of mature osteoclasts, 3) altering the life span of differentiated and mature osteoclasts (Baron *et al.*, 2011; Reszka and Rodan, 2003). Currently, bisphosphonates (*e.g.* alendronate, risedronate and zoledronate) are the most commonly used antiresorptive therapy. Bisphosphonates bind to the mineral component of bone and are taken up by osteoclasts during bone resorption. Inside the osteoclast, bisphosphonates work through intercellular mechanisms to inhibit osteoclast function and survival (Reszka and Rodan, 2003). Denosumab is another anti-resorptive treatment that impedes osteoclastogenesis and osteoclast activity by disrupting the RANK/RANKL pathway. As a monoclonal antibody that targets RANKL, denosumab prevents RANKL from binding to its receptor RANK, thereby inhibiting osteoclast formation, activity and survival (Baron *et al.*, 2011; Hanley *et al.*, 2012).

The effectiveness of both bisphosphonates and denosumab to minimise bone loss is reflected in their ability to significantly reduce the activation of new BMUs (Chavassieux *et al.*, 1997; Dempster *et al.*, 2018; Kostenuik *et al.*, 2015; Recker *et al.*, 2008; Reid *et al.*, 2010). Compared to treatment-naive postmenopausal women, a 3-year treatment with bisphosphonates reduced activation frequency 2.7-fold (Recker *et al.*, 2008). Similarly, activation frequency was 6.7-fold lower in postmenopausal women treated with denosumab for 5 years (Brown *et al.*, 2014). The reduction in bone loss associated with bisphosphonate treatment is largely attributed to this attenuated turnover rate, as the erosion depth in trabecular bone (Chavassieux *et al.*, 1997; Eriksen *et al.*, 2002) and cortical bone (Bernhard *et al.*, 2013) was similar between control subjects and those treated with bisphosphonates. On the other hand, denosumab has been shown to reduce the erosion depth of BMUs in trabecular bone by approximately 30 % (Chavassieux *et al.*, 2019b). This may partly explain why improvements in total and cortical bone mineral density with denosumab were superior to those caused by alendronate (Brown *et al.*, 2009; Seeman *et al.*, 2010), although how much resorption is limited by denosumab at the BMU-level has yet to be investigated in cortical bone (*e.g.* osteon diameter).

Following the theory that BMU activity is normally tightly coupled, modifying bone resorption would consequently alter bone formation (Chavassieux *et al.*, 1997; Jensen *et al.*, 2021); however, change in bone formation after anti-resorptive drugs, as evidenced by histomorphometry, is convoluted. Wall thickness was unchanged following 1-3 years of treatment with bisphosphonates (Chavassieux *et al.*, 1997; Eriksen *et al.*, 2002) or denosumab (Chavassieux *et al.*, 2019b; Reid *et al.*, 2010) but the proportion of mineralising surface was significantly reduced with both drugs (Chavassieux *et al.*, 1997; Chavassieux *et al.*, 2019b; Eriksen *et al.*, 2002; Reid *et al.*, 2010). In addition, inconsistent changes in mineral apposition rate following bisphosphonate and denosumab treatment have been reported. After 2 and 3 years of alendronate and risedronate treatment, respectively, mineral apposition rate was marginally lower than in controls, although this difference was not significant (Chavassieux *et al.*, 1997; Eriksen *et al.*, 2002). In contrast, others report that mineral apposition rate was slightly higher after 1, 2 or 3 years of alendronate treatment compared to placebo (Bone *et al.*, 1997; Chavassieux *et al.*, 1997) and significantly increased after 3 years of zoledronic acid treatment (Recker *et al.*, 2008). Regarding denosumab, Reid *et al.* (2010) found mineral apposition rate to be reduced after 2 and 3 years of treatment, although some have demonstrated that the decreased mineral apposition rate observed at 2 years returned toward rates observed in placebo groups by 3 years (Chavassieux *et al.*, 2019b).

Future experimental opportunities

These examples of disrupted or modified bone remodelling illustrate how delicate the remodelling process can be, in which altering a single factor may dismantle the tight coupling and balance of BMUs. They also provide a unique opportunity to evaluate current hypotheses of the remodelling process and better understand the phases and coupling mechanisms of BMU activity.

The activation-resorption-formation sequence was first described by Frost (Frost, 1969) and is now referenced so frequently to describe the remodelling process one may have the illusion that the regulation and activity in each of these phases is well understood. On the contrary, there remain several open questions, especially concerning cortical bone and its activation, resorption and formation.

- What governs the frequency and spatial distribution of BMU origination?
- What dictates reversal from bone resorption to formation (*i.e.* coupling mechanisms)?
- How might this mechanism(s) be disrupted and/or restored?
- How do the spatial and temporal characteristics of BMU activity ultimately affect the structure and function of the whole bone?

The sections that follow discuss current and future experimental opportunities that may help address these questions, challenge existing theoretical frameworks of bone remodelling regulation and dynamics, and ultimately improve the understanding of the spatio-temporal behaviour of BMUs.

3D morphological analysis of BMU remodelling spaces

Osteon morphology is a direct reflection of BMU osteoclastic and osteoblastic activity and measurements of osteon diameter and wall thickness are currently the best estimates of the amount of bone resorbed and formed during an individual remodelling event. These inherently 2D static measures are heavily dependent on the timing and specific slice selected for analysis, capturing the output of a BMU within a limited timeframe and at a single location. Serial sectioning has provided novel insights into the 3D morphology of osteons; however, these techniques are challenging and only few studies have used this approach to investigate intracortical bone microarchitecture (Cohen and Harris, 1958; Lassen *et al.*, 2017; Robling and Stout, 1999; Stout *et al.*, 1999; Tappen, 1977). Quantifying the 3D shape of remodelling spaces, which is more accessible through X-ray-based imaging (Fig. 3), may help elucidate the spatio-temporal behaviour of BMUs, specifically the capacity of the resorption and formation phases and how reversal mechanisms mediate their relationship.

X-ray μCT is the gold standard for non-destructive 3D analysis of trabecular microarchitecture and is increasingly being used to investigate that of cortical bone (Basillais *et al.*, 2007; Cooper *et al.*, 2003; Cooper *et al.*, 2007; Cooper *et al.*, 2011; Pazzaglia *et al.*, 2009). There are many benefits of using μCT compared to histology-based methods, including 1) a larger field of view that is not limited to a 2D section and its orientation, 2) BMU remodelling spaces may be observed directly without interpolating 2D sections, 3) the amount of bone resorbed and formed can be calculated as a volume rather than as an area. Furthermore, μCT is a promising approach for imaging BMU-related resorption cavities as their larger size and distinctive cutting cones are discernibly different from the smaller canals of completed osteons. Recent work has demonstrated the feasibility of such methods by using μCT to identify BMUs in a rabbit tibia *ex vivo* without the need for additional histological sectioning (Harrison *et al.*, 2020a).

Building on this work, 3D analysis of remodelling space morphology would provide more comprehensive measurements of each remodelling phase. The radius and length of the cutting cone, reversal zone or closing cone would be indicative of the change in volume within each phase, while the slope signifies the radial rate of change in bone tissue (Fig. 4). Unlike measurements derived from classic histological techniques, a 3D analysis of BMU-related resorption cavities would afford direct assessment of the resorption phase and its spatial relationship with formative activity. Quantifying 3D remodelling space morphology would be particularly useful when detection of fluorochrome labels is unreliable, such as with glucocorticoid treatment, because remodelling spaces could be identified independent of formative activity.

In addition, a morphological analysis could be used to challenge paradigms surrounding remodelling dynamics. The conventional concept of bone remodelling depicts BMU activity as a sequential order of events, *i.e.* activation-resorption-formation (Frost, 1969), and describes the reversal phase between resorption and formation as a quiescent zone with no resorptive or formative activity (Parfitt, 1982). If this were the case, the slope of the cutting cone would initially increase and then plateau during the quiescent reversal period (Fig. 5**a**). However, recent developments suggest that the reversal phase involves mixed reversal-resorption activity, during which bone continues to be resorbed (radially) and the switch from bone resorption to formation is driven by cellular expansion of osteoprogenitor cells (Lassen *et al.*, 2017). In this instance, both the cutting cone and reversal zone would have a non-zero slope (Fig. 5**b**) and clearly illustrate a different reversal mechanism from the conventional remodelling paradigm. Furthermore, variation in BMU shape may elucidate the effects of different interventions on remodelling dynamics. For example, both denosumab and bisphosphonate treatments reduce activation frequency, while resorption volume for a given BMU may only be effectively reduced with denosumab treatment (Fig. 4**b**). Similarly, remodelling is thought to be uncoupled with glucocorticoid treatment and ongoing resorption or an arrested reversal zone would be evident in altered remodelling space morphology (Fig. 4**b**).

Beyond quantitative measures of remodelling space morphology, qualitative descriptions vary widely in the literature. Most notably, the nature of the reversal zone and the shape of the cutting cone, which has been depicted as a pointed (Jaworski *et al.*, 1972; Parfitt, 1994; Robling and Stout, 1999) or spherical cone (Roberts *et al.*, 1984; Roberts *et al.*, 2006). These seemingly minute changes in morphology may actually represent meaningful differences in remodelling dynamics that are currently unappreciated. Furthermore, computational models of BMU activity typically rely on idealised, often 2D, representations of BMU morphology (Buenzli *et al.*, 2012; Buenzli *et al.*, 2014; Burger *et al.*, 2003; van Oers *et al.*, 2008a; Smit and Burger, 2000) even though irregular morphologies were reported over 50 years ago (Johnson, 1964; Tappen, 1977) and complex 3D morphologies have been reported more recently (Cooper *et al.*, 2011; Maggiano *et al.*, 2016). Varying BMU shape would likely change the results and interpretation of these models, highlighting the importance of investigating and reporting accurate BMU morphologies.

4D time-lapsed *in vivo* analysis of BMU remodelling spaces

Although morphological analysis of data already available with *ex vivo* 3D imaging has the potential to expand the understanding of BMU activity, detecting and tracking BMUs over time (4D) *in vivo* would provide novel insights into remodelling dynamics. Longitudinal *in vivo* μCT studies have successfully tracked changes in trabecular bone architecture, quantifying the alterations in thickness, separation and number of individual trabeculae due to age, disease and therapeutic interventions (de Bakker *et al.*, 2015; David *et al.*, 2003; Waarsing *et al.*, 2004). Technical challenges, including the high-resolution requirements and radiation concerns, have hindered such *in vivo* analyses in cortical bone; however, recent advances in imaging technology present an

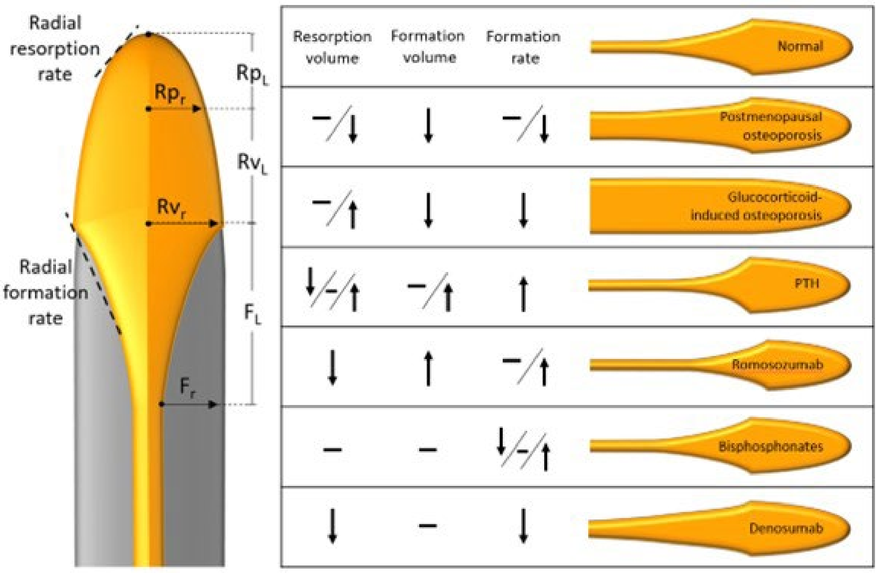

Fig. 4. **Theoretical variations in BMU morphology.** Schematic representation of 3D morphological measures of BMU-related remodelling space, including radius (r) and length (L), and slope of the resorption (Rp), reversal (Rv) and formation (F) phases, that could be used to calculate the amount and radial rate of change in bone tissue. The table summarises changes in BMU activity in osteoporosis and with pharmaceutical treatments and poses hypothetical shapes of remodelling spaces that may reflect an altered remodelling event. Changes relative to normal BMU activity: no change (-), increased (↑), decreased (↓), inconclusive and maybe increased, decreased or no change (↓/-/↑).

opportunity for innovative methods to investigate cortical bone remodelling *in vivo* and longitudinally. Conventional μCT imaging can detect cortical porosity in animal models *in vivo* (Altman *et al.*, 2015; Li *et al.*, 2015) but the high radiation dose associated with increased resolution makes the characterisation of individual BMUs currently beyond reach. Advantages of SR μCT, such as increased resolution and contrast, along with reduced scan times, offer a potential avenue for *in vivo* imaging of remodelling events in animal models (Harrison and Cooper, 2015). Pratt *et al.* (2015) demonstrated that SR μCT could resolve cortical pores in rat tibia without a considerable increase in radiation dose (dose = 2.53 Gy, voxel resolution = 11.8 μm) compared to laboratory μCT (dose = 1.2-1.5 Gy, voxel resolution = 18 μm; dose = 11.7-18.2 Gy, voxel resolution = 9 μm). In addition, utilising SR μCT in larger-animal models that exhibit larger cortical pores, such as rabbits, would ease the resolution requirements and further reduce the radiation dose. Beyond animal models, HR-pQCT is being used increasingly to investigate cortical porosity in human bone *in vivo* (Britz *et al.*, 2012; Chen *et al.*, 2010; Cooper *et al.*, 2003; Cooper *et al.*, 2006; Pazzaglia *et al.*, 2009). With an isotropic voxel size of 82 μm, the size of a single voxel is on the same scale as the average canal diameter in human cortical bone [~ 80-120 μm (Cooper *et al.*, 2007; Particelli *et al.*, 2012)] and HR-pQCT is likely unable to resolve all canals (Jorgenson *et al.*, 2015; Soltan *et al.*, 2019). However, remodelling spaces are ~ 220-245 μm in diameter on average (Britz *et al.*, 2009; Jowsey, 1966), suggesting that HR-pQCT can potentially detect and track individual remodelling events in human bone.

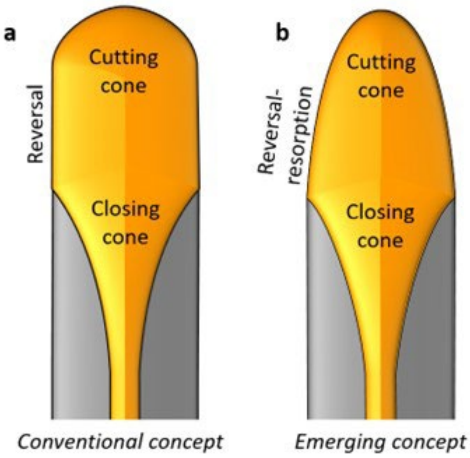

Fig. 5. Morphology of BMU-related remodelling spaces has the potential to elucidate differences in BMU activity and challenge to hypotheses of remodelling dynamics. (**a**) Conventional framework of remodelling process in which the reversal phase is transition zone between resorption and formation with limited activity. (**b**) Emerging concept of remodelling dynamics that suggests resorption continues throughout the reversal zone and plays a role in the transition to bone formation.

Non-destructive imaging modalities, such as μCT, allow multiple *in vivo* scans of the same bone. Comparing sequential images can elucidate changes occurring over time, such as spatial and temporal changes in bone resorption and formation. To evaluate these longitudinal changes, follow-up images need to be accurately aligned with the baseline image. Such image registrations techniques have been developed and are routinely used for quantifying longitudinal changes in trabecular bone (Boyd *et al.*, 2006; Christen and Müller, 2017; Waarsing *et al.*, 2004). Typically, a rigid body registration uses an optimisation algorithm, translating and rotating the images onto each other, to find the transformation that aligns the images to the satisfaction of a given objective function. Then, the transformation is applied and interpolation is used on the follow-up image to assign each voxel its new coordinates. Superimposing registered images can reveal differences between sequential images and may generally be interpreted as follows: bone that is present in only the first image is considered to be resorbed by the follow-up image, while bone that only appears in the follow-up image corresponds to newly formed bone. Bone that exists in both images is considered as quiescent, unchanged bone.

The chosen objective function may be feature- or voxel-based and intends to maximise the similarity between the images. A feature-based approach attempts to minimise the distance between corresponding features in the two images. Given the dynamic structural changes in bone, feature-based registration can be problematic, as features in the first scan may be unrecognisable (*e.g.* absent or significantly altered) by the follow-up scan. Voxel-based registration uses similarity metrics such as grey-scale intensity values, normalised correlation

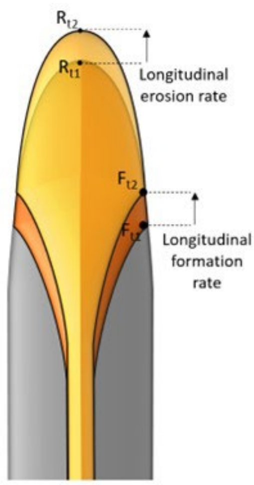

Fig. 6. Schematic representation of 4D time-lapsed analysis of BMU-related remodelling spaces. Schematic representation of 4D time-lapsed analysis of BMU activity to track the resorption (R) and formation (F) front at multiple timepoints (t1 and t2). Direct assessment of BMU advance enables the calculation of longitudinal erosion and formation rates.

or mutual information to determine the degree of shared information, or overlap, of the two images. Voxel-based registration is most frequently used in trabecular bone studies due to its robustness and accuracy (Rueckert and Schnabel, 2011). In fact, remodelling parameters in mice vertebrae following µCT image registration were shown to be highly reproducible with interclass correlation coefficients as high as 0.965 for eroded surface and 0.991 for mineral apposition rate (a coefficient of 1 indicates perfect reproducibility) (Schulte *et al.*, 2011a) and strongly correlated with traditional histological measurements (Birkhold *et al.*, 2014; Schulte *et al.*, 2011a).

Recent work by Harrison and colleagues has demonstrated the feasibility of using correlation and normalised mutual information metrics in registering and tracking cortical bone remodelling [Harrison K *et al.* (2020b) Direct four-dimensional assessment of cortical bone basic multicellular unit longitudinal erosion rate in PTH-dosed rabbits: a novel synchrotron X-ray imaging approach. Conference abstract, 42nd meeting of the American Society of Bone and Mineral Research]. Compared to trabecular bone, registering sequential images of cortical bone has the added advantage of more distinct stable structures that may aid in feature-based registration. The vascular canals permeating cortical bone, for example, provide unchanged (relative to the imaging or experimental time frame) structures that, at the very least, can highlight the success of image registration visually and, at most, potentially be used as fiducial-like markers in a feature-based registration (Fig. 7). Another challenge of 4D imaging that persists regardless of bone type or registration metric is the temporal resolution. This is not a method for observing changes in real time. Similar to histology or 3D imaging techniques, each follow-up image illustrates the bone's state at a discrete point in time. Follow-up images need to be taken at long enough intervals to capture meaningful and measurable change but not so long that information is lost. The timing of scans and duration of experiments will only be realised with more research and will be specific to the imaging modality, the animal model of interest and the impetus of the study.

One of the most notable benefits of imaging BMU activity *in vivo*, either animal models using SR µCT or human bone using HR-pQCT, is the ability to track BMUs over multiple time points. These techniques would elucidate the progression of BMUs, both the trajectory and rate of change in bone tissue, across the remodelling phases (Fig. 6). Additionally, 4D analysis provides an opportunity to measure aspects of resorptive activity, including erosion period and rate (Harrison *et al.*, 2020b), which are commonly reported in histological studies but indirectly inferred from bone formation activity. In particular, the longitudinal erosion rate (*i.e.* cutting cone advance) has been measured based on the assumption that the cutting cone progression is equal to that of the closing cone (Jaworski and Lok, 1972; Takahashi *et al.*, 1971). Given the possibility for imbalanced and uncoupled BMU activity, synchronised phases cannot be assumed. Longitudinal assessment of remodelling may also push past limitations of the typical 2D analysis of activation frequency by identifying new remodelling sites within a larger volume and defined time frame, rather than depending on formation indices in a small cross-sectional field of view. Finally, the greatest impact of 4D *in vivo* analysis is its potential to investigate and optimise dosing regimens of existing and future treatments. If the resorption rate and size of BMUs could be reduced, tightly coupled with formation, and spatially controlled to prevent merging with other pores, then bone loss could be minimised or even reversed. *In vivo* investigation of BMU activity in 4D is the next step towards clarifying the spatio-temporal coordination of BMUs in cortical bone and the first step towards targeted manipulation of bone remodelling.

In silico modelling

Many mathematical models synthesise mechanical and biological information in an attempt to simulate bone turnover at the whole bone, tissue and cellular

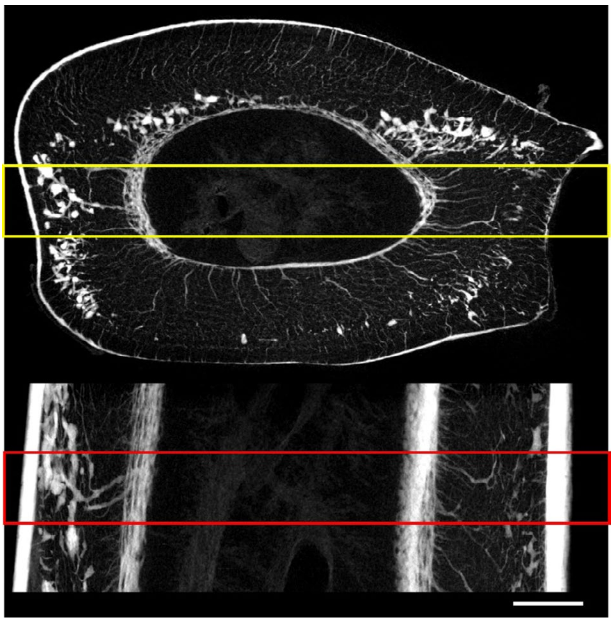

Fig. 7. Stable structures visible in cortical bone that may facilitate image registration. A cross-sectional (top) and longitudinal (bottom) standard deviation projection of a rabbit tibia dosed with PTH (see Fig. 2 for a 3D view of the corresponding rabbit tibia). Even with the considerable amount of remodelling activity associated with PTH, stable Haversian canals throughout the cortex are detectable. As unchanged structures, the canals may provide fiducial-like markers in cortical bone and aid in feature-based registration routines. The 1 mm region used to create the cross-sectional and longitudinal projections is contained within the red and yellow box, respectively. Data and images courtesy of Dr Kim Harrison (Harrison *et al.*, 2020a) (scale bar = 1 mm).

level (Defranoux *et al.*, 2005; Kameo *et al.*, 2020; Pivonka and Komarova, 2010). With respect to the remodelling process, mathematical modelling may be particularly advantageous in identifying parameters that significantly alter BMU behaviour and contribute to consequential changes in overall cortical porosity. Smith *et al.* (2012) created a theoretical framework in which differential changes in bone volume can be described by the control mechanisms that govern bone resorption and formation. Of interest, the rate of BMU progression was found to play a role in maintaining local bone volume. This is encouraging from a therapeutic perspective as a potential target that may be manipulated to remedy dysfunctional remodelling. Mathematical models are also useful in quantifying the relationship between changes in tissue and organ level properties. It may seem intuitive that increased activation frequency and larger canal diameters contribute to increased porosity (Martin, 1991); however, models can help identify not only which of these variables play a role in the overall process, but also the level of variability in these parameters required to elicit meaningful change in tissue and organ level properties.

Advances in experimental techniques and substantial growth of available data have provided more accurate estimates of initial conditions and parameters as well as a better understanding of the governing biological processes, all of which inform more sophisticated and relevant models. Models of the spatio-temporal behaviour of BMUs are becoming increasingly complex by integrating mechanical, biochemical and cellular signalling dynamics to capture the physiological features of the remodelling process (Buenzli *et al.*, 2011; Martínez-Reina *et al.*, 2009; Ryser *et al.*, 2009). Model-informed drug development is also not a new concept but a model's usefulness and applicability rely on rigorous validation to ensure the results correspond to the physical reality and specific context of interest. Unfortunately, data on tissue-level remodelling parameters of human cortical bone are scarce (Table 1). Additionally, as mentioned previously, what is known about the cellular activity is not always evident in histological observations at the tissue level. This limits further the development of accurate and comprehensive models as well as the validation of model predictions. When defining a model, it is not enough to describe osteoclastic activity as enhanced, for example, but rather an explicit value or function is needed to define such activity. The proposed 3D and 4D morphological analysis of BMUs could provide data to improve model definitions and the means to test hypotheses generated by mathematical models regarding the spatial and temporal regulation of BMUs.

While mathematical models are well-suited to explore the relevance of remodelling variables and their relationship across multiple scales, computational models are typically used to investigate the effects of external factors on the parameters and outcomes of bone remodelling. A large body of research has focused on the mechano-regulation of bone adaptation, using computational models to explain the link between the mechanical environment and remodelling activity. In general, the theory of these models is based on the mechanosensory role of osteocytes, converting a mechanical stimulus into biochemical signals that may stimulate osteoblasts and/or inhibit osteoclasts. Simulations of various loading magnitudes, frequencies, directions and gradients have been shown to govern BMU trajectories (Martínez-Reina *et al.*, 2009; van Oers *et al.*, 2008a), the cutting cone diameter (*i.e.* osteon diameter) (van Oers *et al.*, 2008b), BMU morphology (van Oers *et al.*, 2008b), microarchitectural organisation (Hambli, 2014; Mullender and Huiskes, 1995; Tsubota *et al.*, 2009), BMU coupling (Smit *et al.*, 2002; Smit and Burger, 2000) and mineral density (Berli *et al.*, 2017; Hambli, 2014). van Oers *et al.* (2008b) presented a 2D model that suggested osteon diameter is related to strain magnitude, with lower strains resulting in larger osteons. Their model also predicted that BMUs progressed parallel to the principal loading direction, but in the absence of mechanical loading, osteoclasts did not form an organised cutting cone and followed arbitrary paths. These findings are consistent with the unrestrained resorption activity observed in immobilised primates, where resorption cavities were 5 times larger than normal (500-1,500 μm) (Young *et al.*, 1986), and the lack of microarchitectural organisation following hindlimb unloading in rats (Britz *et al.*, 2012). While it is tempting to draw parallels between model predictions and altered remodelling in certain pathologies (*e.g.* disuse osteoporosis), caution should be exercised when interpreting results from such 2D models. If strain plays a central role in remodelling, the irregular morphology and branching patterns of BMUs may create strain patterns that cannot be captured in simplified 2D models. 3D models of BMU trajectory and microarchitecture orientation seemingly confirm a link between mechanical stimuli and BMU progression (Martínez-Reina *et al.*, 2009; Martínez-Reina *et al.*, 2014) but validation with *in vivo* experimental data in cortical bone is currently limited.

Recent innovations in imaging and computational models have the potential to improve the understanding of mechano-regulated bone remodelling. A significant development is the longitudinal study of bone adaptation using time-lapsed imaging, which allows previously unattainable temporal parameters of remodelling, including resorption volume and rate. Measures of mineral apposition rate also benefit from the 3D nature and larger field of views inherent to μCT imaging (Schulte *et al.*, 2011a). Moreover, the combination of time-lapsed imaging and FE models is being used increasingly to explain the link between mechanical loading and bone remodelling in trabecular bone. Using *in vivo* μCT and FE models of

Table 1. Known parameters of BMU activity for human cortical bone. Resorption values from histomorphometry studies were not included as these are indirectly inferred from markers of bone formation. Ct.Po = cortical porosity; Ac.f = activation frequency; - = the parameter was not reported; On.MAR = osteonal mineral apposition rate; On.Dia = osteon diameter; On.W.Th = osteon wall thickness.

Reference	Population	Anatomical location	Ct.Po (%)	Ac.f (#/yr)	On.MAR (μm/day)	On.Dia (μm)	On.W.Th (μm)
Normal							
Qiu *et al.* (2020)	Premenopausal women	Trans-iliac crest	-	0.415	0.623	37.5	-
Bernhard *et al.* (2013)	Young females	Femur diaphysis	-	-	-	88.55	233.14
Bernhard *et al.* (2013)	Aged females	Femur diaphysis	-	-	-	66.63	193.35
Osteoporosis							
Chavassieux *et al.* (2019a)	Postmenopausal women w/OP	Trans-iliac crest	4.36	-	0.64	-	-
Chavassieux *et al.* (2019b)	Postmenopausal women w/OP	Trans-iliac crest	6.43	-	0.62	-	-
Bernhard *et al.* (2013)	Treatment-naïve women w/OP	Femur diaphysis	-	-	-	53.05	179.7
Glucocorticoid-induced osteoporosis							
Vedi *et al.* (2005)	Premenopausal women and men	Trans-iliac crest	8.43	0.439	0.59	48.8	-
Teriparatide							
Dempster *et al.* (2016)	Postmenopausal women w/OP	Trans-iliac crest	9.62	-	0.75	-	-
Romosozumab							
Chavassieux *et al.* (2019a)	Postmenopausal women w/OP	Trans-iliac crest	3.83	-	0.61	-	-
Bisphosphonates							
Dempster *et al.* (2016)	Postmenopausal women w/OP	Trans-iliac crest	5.64	-	0.46	-	-
Bernhard *et al.* (2013)	BP-treated women w/OP	Femur diaphysis	-	-	-	74.94	215.78
Denosumab							
Chavassieux *et al.* (2019b)	Postmenopausal women w/OP	Trans-iliac crest	5.9	-	0.59	-	-

mice vertebra, Shulte *et al.* (2013a) demonstrated that globally applied loads control bone resorption and formation at the tissue level. Bone resorption occurred at sites of low strain while bone formation occurred in areas of high strain. Similar methods have also been used to investigate the mechanosensitivity of the remodelling response with age and osteoporosis (Birkhold *et al.*, 2014; Lambers *et al.*, 2012; Lambers *et al.*, 2015). Interestingly, the mechanosensitivity of osteoporotic mice was reduced compared to controls and exhibited an increased amount of non-targeted remodelling (*i.e.* resorption occurring irrespective of the level of mechanical stimuli at that location) (Lambers *et al.*, 2012). *In vivo* data from these longitudinal mice studies were used to validate an *in silico* model simulating the anabolic process associated with mechanical loading. The model successfully predicted changes in bone volume fraction with less than 2.45 % error compared to longitudinal experimental data but could not emulate the dynamic parameters of remodelling, including mineral apposition rate, resorption rate, mineralising surface and erosion surface (Schulte *et al.*, 2011b).

The integration of time-lapsed imaging and FE models has generated similar insights into the mechano-regulation of remodelling in endocortical bone (Birkhold *et al.*, 2015) but has yet to be implemented to study intracortical bone. With the possibility of longitudinal *in vivo* imaging, future models of cortical bone may consider more realistic and variable BMU morphologies in the context of their 3D surroundings to better understand how the local mechanical environment might govern BMU progression. The observation that osteons are generally aligned with the principal loading direction (Heřt *et al.*, 1994; Petrtýl *et al.*, 1996) has engendered the widely accepted theory that BMU trajectories are guided by mechanical stimuli without direct evidence of BMU progression responding to known loading conditions. Furthermore, the inability of previous *in silico* models to predict spatial patterns of bone resorption and formation (Schulte *et al.*, 2013b; 2013a) suggests a local feedback mechanism exists that determines if bone is formed or resorbed in a site-specific manner. If so, local strain concentrations surrounding pores and osteon boarders would make important contributions to the mechano-regulation of BMUs. FE models, including intracortical microarchitecture, are needed to reveal the complex strain distributions associated with the intricate network of Haversian systems. Beyond understanding the influence of mechanical environment on intracortical remodelling, time-lapsed imaging of cortical BMUs can provide the empirical data to derive and validate *in silico* models of altered bone remodelling in disease states or by pharmaceutical treatments in a way that was not possible before. Successful models will greatly increase the rate of research discovery as a platform to test existing and future treatments. Treatment strategies may be modelled and manipulated iteratively *in silico* with promising outcomes then being tested experimentally.

Hybrid imaging approaches

Fluorochrome labelling of bone formation was pioneered 60 years ago (Frost *et al.*, 1961) and remains the standard technique to examine and quantify dynamic parameters of bone remodelling. While this is not without reason, there is potential to combine histology with non-destructive imaging techniques (*e.g.* μCT), such as CT-guided histology or end-point histology, to alleviate some of the limitations of both modalities and gain novel insights into bone remodelling. Many studies already include both histology and μCT methods and the findings are presented as complementary, yet separate measures. CT-guided histology may be the next step for truly integrating these techniques. Capturing active remodelling sites in thin histological sections is fortuitous and, if observed, the state of the BMU can be difficult to discern in a transverse cross-section. A longitudinal section through a BMU (Fig. 3**a**) helps identify the presence, sequence and spatial relationship of cells throughout the different phases of remodelling but, due to the semi-random and oblique orientation of BMUs, precise longitudinal sectioning is challenging and rarely reported in the literature (Lassen *et al.*, 2017; Schenk and Willenegger, 1964). As a non-destructive technique, μCT could be used to locate remodelling sites and guide the histological sectioning of individual BMUs. Recently, a method for merging histological and μCT images of bone lesions in the femoral head was developed (Mourad *et al.*, 2018), but the potential of such techniques in bone remodelling analysis has yet to be realised. End-point histology would also serve to validate information from 3D imaging. For instance, the 3D morphological analysis proposed herein would assume that the identifiable physical features of a BMU are associated with changes in cellular activity (*e.g.* a change in slope may be defined as the beginning or end of the resorption or formation phase). Measurements of osteoid formation or the presence of specific cells in the corresponding histological slice would serve to validate the morphological analysis and inform more realistic assumptions for 3D-based assessments.

Beyond measures of vascular porosity captured using conventional X-ray μCT, SR μCT may provide insight into the dynamics of bone remodelling. Phase contrast leverages the differences in X-ray refractive indices within a target sample to enhance image contrast and reveal small variations in tissue mineralisation that would otherwise be muted with conventional absorption-based X-ray imaging. In bone, this technique is particularly well-suited for the segmentation of secondary osteons (Gauthier *et al.*, 2019; Maggiano *et al.*, 2016). Maggiano *et al.* (2016) used phase contrast to delineate the cement line of individual osteons (Fig. 3**d**) and illustrated the inter-connected network of Haversian systems in 3D, a level of complexity that was previously underappreciated. With regards to remodelling activity, the connectivity and branching patterns of osteons noted by Maggiano *et al.* (2016) gives new insight on the activation site and trajectory of BMUs. The ability to visualise cement lines in 3D also presents an opportunity to investigate unknown parameters of BMU behaviour, such as asymmetric resorption and formation activity that may lead to "drifting osteons" (Robling and Stout, 1999) or the size of the cutting cone over the lifetime of the BMU. Another exciting development on the horizon is the dynamic labelling of bone formation in 3D through K-edge subtraction. The linear attenuation coefficient of an element is a function of the X-ray energy and a sudden change in the linear attenuation coefficient will occur when the X-ray energy is equal to or greater than the binding energy of the K-shell electron. The K-edge subtraction technique exploits this element-specific attenuation discontinuity by imaging above and below the K-edge energy to detect and map a single element of interest. Elements such as barium and strontium are incorporated into newly formed bone, similar to tetracyclines, and have shown potential as labels of bone formation in 3D. K-edge subtraction of strontium labels in the vertebrae of OVX rats indicated periosteal bone formation and trabecular remodelling (Cooper *et al.*, 2012). Similarly, barium was detected in areas of new bone formation in growing rats, including the epiphyses and metaphyses of the femur and tibia as well as the newly forming trabeculae and periosteal cortical bone throughout the diaphysis (Panahifar *et al.*, 2016). Although K-edge subtraction has yet to be applied to cortical bone remodelling, *in vivo* 3D labels of bone formation could support the aforementioned time-lapsed analysis of BMU activity and elucidate the radial and longitudinal rate of bone formation.

Conclusions

Despite its central role in bone adaptation and disease, the spatio-temporal organisation of BMUs in cortical bone has never been directly observed *in vivo*. Hence, the 3D and 4D coordination of BMU behaviour is unknown. This knowledge gap is attributed to limited imaging capabilities but advances in imaging technology, such as *in vivo* SR imaging, present new opportunities to investigate BMU activity. A 3D morphological analysis of BMU-related remodelling spaces offers meaningful and accessible measurements that are telling of BMU activity and would provide novel insights into remodelling dynamics that may challenge existing paradigms and enlighten new perspectives on the remodelling process. Additionally, developing *in vivo* imaging methods to track remodelling spaces over time (4D) is an exciting opportunity on the horizon that will enable direct assessment of BMU advance. Such techniques will help clarify how bone resorption and formation are spatially and temporally synchronised as well as the impact of interventions such as pharmaceutical treatments. Developing *in silico* models that correspond with this novel empirical data is a crucial component in the experimental-theoretical pipeline in which new treatment strategies may be iteratively modelled, manipulated, optimised and experimentally tested to accelerate research discovery and clinical impact.

References

Adami G, Saag KG (2019) Glucocorticoid-induced osteoporosis update. Curr Opin Rheumatol **31**: 388-393.

Aguirre JI, Plotkin LI, Stewart SA, Weinstein RS, Parfitt AM, Manolagas SC, Bellido T (2006) Osteocyte apoptosis is induced by weightlessness in mice and precedes osteoclast recruitment and bone loss. J Bone Miner Res **21**: 605-615.

Altman AR, Tseng WJ, de Bakker CMJ, Chandra A, Lan S, Huh BK, Luo S, Leonard MB, Qin L, Liu XS (2015) Quantification of skeletal growth, modeling, and remodeling by *in vivo* micro computed tomography. Bone **81**: 370-379.

Andersen TL, Abdelgawad ME, Kristensen HB, Hauge EM, Rolighed L, Bollerslev J, Kjærsgaard-Andersen P, Delaisse JM (2013) Understanding coupling between bone resorption and formation: are reversal cells the missing link? Am J Pathol **183**: 235-246.

Andreasen CM, Ding M, Overgaard S, Bollen P, Andersen TL (2015) A reversal phase arrest uncoupling the bone formation and resorption contributes to the bone loss in glucocorticoid treated ovariectomised aged sheep. Bone **75**: 32-39.

Andreasen CM, Delaisse J-M, van der Eerden BC, van Leeuwen JP, Andersen TL (2018) Understanding age-induced cortical porosity in women: the accumulation and coalescence of eroded cavities upon existing intracortical canals is the main contributor. J Bone Miner Res **33**: 606-620.

Arlot ME, Delmas PD, Chappard D, Meunier PJ (1990) Trabecular and endocortical bone remodeling in postmenopausal osteoporosis: comparison with normal postmenopausal women. Osteoporos Int **1**: 41-49.

Aslan D, Andersen MD, Gede LB, De Franca TK, Jørgensen SR, Schwarz P, Jørgensen NR (2012) Mechanisms for the bone anabolic effect of parathyroid hormone treatment in humans. Scand J Clin Lab Invest **72**: 14-22.

Bakker A, Klein-Nulend J, Burger E (2004) Shear stress inhibits while disuse promotes osteocyte apoptosis. Biochem Biophys Res Commun **320**: 1163-1168.

de Bakker CMJ, Altman AR, Tseng WJ, Tribble MB, Li C, Chandra A, Qin L, Liu XS (2015) μCT-based, *in vivo* dynamic bone histomorphometry allows 3D evaluation of the early responses of bone resorption and formation to PTH and alendronate combination therapy. Bone **73**: 198-207.

Balani DH, Ono N, Kronenberg HM (2017) Parathyroid hormone regulates fates of murine osteoblast precursors *in vivo* **127**: 3327-3338.

Baron R, Ferrari S, Russell RGG (2011) Denosumab and bisphosphonates : different mechanisms of action and effects. Bone **48**: 677-692.

Basillais A, Bensamoun S, Chappard C, Brunet-Imbault B, Lemineur G, Ilharreborde B, Ho Ba Tho MC, Benhamou CL (2007) Three-dimensional characterization of cortical bone microstructure by microcomputed tomography: validation with ultrasonic and microscopic measurements. J Orthop Sci **12**: 141-148.

Bell KL, Loveridge N, Reeve J, Thomas CDL, Feik SA, Clement JG (2001) Super-osteons (remodeling clusters) in the cortex of the femoral shaft: influence of age and gender. Anat Rec **264**: 378-386.

Berli M, Borau C, Decco O, Adams G, Cook RB, Aznar JMG, Zioupos P (2017) Localized tissue mineralization regulated by bone remodelling: a computational approach. PLoS One **12**: 1-19.

Bernhard A, Milovanovic P, Zimmermann EA, Hahn M, Djonic D, Krause M, Breer S, Püschel K, Djuric M, Amling M, Busse B (2013) Micro-morphological properties of osteons reveal changes in cortical bone stability during aging, osteoporosis, and bisphosphonate treatment in women. Osteoporos Int **24**: 2671-2680.

Birkhold AI, Razi H, Duda GN, Weinkamer R, Checa S, Willie BM (2014) The influence of age on adaptive bone formation and bone resorption. Biomaterials **35**: 9290-9301.

Birkhold AI, Razi H, Weinkamer R, Duda GN, Checa S, Willie BM (2015) Monitoring *in vivo* (re) modeling: A computational approach using 4D microCT data to quantify bone surface movements. Bone **75**: 210-221.

Bjørnerem Å (2016) The clinical contribution of cortical porosity to fragility fractures. Bonekey Rep **5**: 1-5.

Bone HG, Downs RW, Tucci JR, Harris ST, Weinstein RS, Licata AA, Clung MRMC, Kimmel DB, Gertz BJ, Hale E, Polvino WJ, The FOR, Elderly A, Study O (1997) Dose-response relationships for alendronate treatment in osteoporotic elderly women. Alendronate Elderly Osteoporosis Study Centers. J Clin Endocrinol Metab **82**: 265-274.

Bonewald LF (2011) The amazing osteocyte. J. Bone Miner. Res. **26**: 229-238. DOI: 10.1002/jbmr.320.

Bord S, Frith E, Ireland DC, Scott MA, Craig JIO, Compston JE (2004) Synthesis of osteoprotegerin and RANKL by megakaryocytes is modulated by oestrogen. Br J Haematol **126**: 244-251.

Boyce BF, Xing L (2007) Biology of RANK, RANKL, and osteoprotegerin. Arthritis Res Ther **9 Suppl 1**: S1. DOI: 10.1186/ar2165.

Boyce RW, Paddock CL, Franks AF, Jankowsky ML, Eriksen EF (1996) Effects of intermittent hPTH (1-34) alone and in combination with 1,25(OH),D, or risedronate on endosteal bone remodeling in canine cancellous and cortical bone. J Bone Miner Res **1**: 600-613.

Boyce RW, Niu QT, Ominsky MS (2017) Kinetic reconstruction reveals time-dependent effects of romosozumab on bone formation and osteoblast function in vertebral cancellous and cortical bone in cynomolgus monkeys. Bone **101**: 77-87.

Boyd SK, Moser S, Kuhn M, Klinck RJ, Krauze PL, Müller R, Gasser JA (2006) Evaluation of three-dimensional image registration methodologies for *in vivo* micro-computed tomography. Ann Biomed Eng **34**: 1587-1599.

Bressot C, Meunier PJ, Chapuy MC, Lejeune E, Edouard C, Darby AJ (1979) Histomorphometric profile, pathophysiology and reversibility of corticosteroid-induced osteoporosis. Metab Bone Dis Relat Res **1**: 303-311.

Britz HM, Thomas CDL, Clement JG, Cooper DML (2009) The relation of femoral osteon geometry to age, sex, height and weight. Bone **45**: 77-83.

Britz HM, Jokihaara J, Leppa O V, Cooper DML (2012) The effects of immobilization on vascular canal orientation in rat cortical bone. J Anat **220**: 67-76.

Brown JP, Prince RL, Deal C, Recker RR, Kiel DP, De Gregorio LH, Hadji P, Hofbauer LC, Álvaro-Gracia JM, Wang H, Austin M, Wagman RB, Newmark R, Libanati C, San Martin J, Bone HG (2009) Comparison of the effect of denosumab and alendronate on BMD and biochemical markers of bone turnover in postmenopausal women with low bone mass: a randomized, blinded, phase 3 trial. J Bone Miner Res **24**: 153-161.

Brown JP, Reid IR, Wagman RB, Kendler D, Miller PD, Erik J, Jensen J-EB, Bolognese MA, Daizadeh N, Valter I, Zerbini CAF, Dempster DW (2014) Effects of up to 5 years of denosumab treatment on bone histology and histomorphometry: the FREEDOM study extension. J Bone Miner Res **29**: 2051-2056.

Brunet S, Sardon T, Zimmerman T, Wittmann T, Pepperkok R, Karsenti E, Vernos I (2004) Characterization of the TPX2 domains involved in microtubule nucleation and spindle assembly in Xenopus nucleation around chromatin and functions in a network of other molecules , some of which also are regulated by. Mol Biol Cell **15**: 5318-5328.

Buenzli PR, Pivonka P, Smith DW (2011) Spatio-temporal structure of cell distribution in cortical bone multicellular units: a mathematical model. Bone **48**: 918-926.

Buenzli PR, Jeon J, Pivonka P, Smith DW, Cummings PT (2012) Investigation of bone resorption within a cortical basic multicellular unit using a lattice-based computational model. Bone **50**: 378-389.

Buenzli PR, Pivonka P, Smith DW (2014) Bone refilling in cortical basic multicellular units: insights into tetracycline double labelling from a computational model. Biomech Model Mechanobiol **13**: 185-203.

Burger EH, Klein-Nulend J, Smit TH (2003) Strain-derived canalicular fluid flow regulates osteoclast activity in a remodelling osteon - a proposal. J Biomech **36**: 1453-1459.

Burr DB, Hirano T, Turner CH, Hotchkiss C, Brommage R, Hock JM (2001) Intermittently administered human parathyroid hormone(1-34) treatment increases intracortical bone turnover and porosity without reducing bone strength in the humerus of ovariectomized cynomolgus monkeys. J Bone Miner Res **16**: 157-165.

Cabahug-Zuckerman P, Frikha-Benayed D, Majeska RJ, Tuthill A, Yakar S, Judex S, Schaffler MB (2016) Osteocyte apoptosis caused by hindlimb unloading is required to trigger osteocyte RANKL production and subsequent resorption of cortical and trabecular bone in mice femurs. J Bone Miner Res **31**: 1356-1365.

Canalis E, Mazziotti G, Giustina A, Bilezikian JP (2007) Glucocorticoid-induced osteoporosis: pathophysiology and therapy. Osteoporos Int **18**: 1319-1328.

Canalis E (1983) Effect of glucocorticoids on type I collagen synthesis, alkaline phosphatase activity, and deoxyribonucleic acid content in cultured rat calvariae. Endocrinology **112**: 931-939.

Carasco MG, de Vernejoul MC, Sterkers Y, Morieux C, Kuntz D, Miravet L (1989) Decreased bone formation in osteoporotic patients compared with age-matched controls. Calcif Tissue Int **44**: 173-175.

Carbonare LD, Arlot ME, Chavassieux PM, Roux JP, Portero NR, Meunier PJ (2001) Comparison of trabecular bone microarchitecture and remodeling in glucocorticoid-induced and postmenopausal osteoporosis. J Bone Miner Res **16**: 97-103.

Charatcharoenwitthaya N, Khosla S, Atkinson EJ, McCready LK, Riggs BL (2007) Effect of blockade of TNF-α and interleukin-1 action on bone resorption in early postmenopausal women. J Bone Miner Res **22**: 724-729.

Chavassieux P, Chapurlat R, Portero-Muzy N, Roux JP, Garcia P, Brown JP, Libanati C, Boyce

RW, Wang A, Grauer A (2019a) Bone-forming and antiresorptive effects of romosozumab in postmenopausal women with osteoporosis: bone histomorphometry and microcomputed tomography analysis after 2 and 12 months of treatment. J Bone Miner Res **34**: 1597-1608.

Chavassieux PM, Arlot ME, Reda C, Wei L, Yates AJ, Meunier PJ (1997) Histomorphometric assessment of the long-term effects of alendronate on bone quality and remodeling in patients with osteoporosis. J Clin Invest **100**: 1475-1480.

Chavassieux P, Portero-Muzy N, Roux JP, Horlait S, Dempster DW, Wang A, Wagman RB, Chapurlat R (2019b) Reduction of cortical bone turnover and erosion depth after 2 and 3 years of denosumab: iliac bone histomorphometry in the FREEDOM trial. J Bone Miner Res **34**: 626-631.

Chen H, Zhou X, Shoumura S, Emura S, Bunai Y (2010) Age- and gender-dependent changes in three-dimensional microstructure of cortical and trabecular bone at the human femoral neck. Osteoporos Int **21**: 627-636.

Christen P, Müller R (2017) *In vivo* Visualisation and quantification of bone resorption and bone formation from time-lapse imaging. Curr Osteoporos Rep **15**: 311-317.

Cohen-Solal ME, Shih M -S, Lundy MW, Parfitt MA (1991) A new method for measuring cancellous bone erosion depth: application to the cellular mechanisms of bone loss in postmenopausal osteoporosis. J Bone Miner Res **6**: 1331-1338.

Cohen J, Harris WH (1958) The three-dimensional anatomy of haversian systems. J Bone Joint Surg Am **40-A**: 419-434.

Cooper DML, Erickson B, Peele AG, Hannah K, Thomas CDL, Clement JG (2011) Visualization of 3D osteon morphology by synchrotron radiation μCT. J Anat **219**: 481-489.

Cooper DML, Thomas CDL, Clement JG, Hallgrimsson B (2006) Three-dimensional microcomputed tomography imaging of basic multicellular unit-related resorption spaces in human cortical bone. Anat Rec **288**: 806-816.

Cooper DML, Thomas CDL, Clement JG, Turinsky AL, Sensen CW, Hallgrimsson B (2007) Age-dependent change in the 3D structure of cortical porosity at the human femoral midshaft. Bone **40**: 957-965.

Cooper DML, Chapman LD, Carter Y, Wu Y, Panahifar A, Britz HM, Bewer B, Zhouping W, Duke MJM, Doschak M (2012) Three dimensional mapping of strontium in bone by dual energy K-edge subtraction imaging. Phys Med Biol **57**: 5777-5786.

Cooper DML, Kawalilak CE, Harrison K, Johnston BD, Johnston JD (2016) Cortical bone porosity: what is it, why is it important, and how can we detect it? Curr Osteoporos Rep **14**: 187-198.

Cooper DML, Turinsky a L, Sensen CW, Hallgrímsson B (2003) Quantitative 3D analysis of the canal network in cortical bone by micro-computed tomography. Anat. Rec. **274**: 169-179.

Cosman F, Crittenden DB, Adachi JD, Binkley N, Czerwinski E, Ferrari S, Hofbauer LC, Lau E, Lewiecki EM, Miyauchi A, Zerbini CAF, Milmont CE, Chen L, Maddox J, Meisner PD, Libanati C, Grauer A (2016) Romosozumab treatment in postmenopausal women with osteoporosis. N Engl J Med **375**: 1532-1543.

Currey JD (1962) Stress concentrations in bone. Q J Microsc Sci **103**: 111-133.

Dalle Carbonare L, Bertoldo F, Valenti MT, Zenari S, Zanatta M, Sella S, Giannini S, Cascio V Lo (2005) Histomorphometric analysis of glucocorticoid-induced osteoporosis. Micron **36**: 645-652.

Darby AJ, Meunier PJ (1981) Mean wall thickness and formation periods of trabecular bone packets in idiopathic osteoporosis. Calcif Tissue Int **33**: 199-204.

David V, Laroche N, Boudignon B, Lafage-Proust MH, Alexandre C, Ruegsegger P, Vico L (2003) Noninvasive *in vivo* monitoring of bone architecture alterations in hindlimb-unloaded female rats using novel three-dimensional microcomputed tomography. J Bone Miner Res **18**: 1622-1631.

Defranoux NA, Stokes CL, Young DL, Kahn AJ (2005) *In silico* modeling and simulation of bone biology: a proposal. J Bone Miner Res **20**: 1079-1084.

Delmas PD, Vergnaud P, Arlot ME, Pastoureau P, Meunier PJ, Nilssen MHL (1995) The anabolic effect of human PTH (1-34) on bone formation is blunted when bone resorption is inhibited by the bisphosphonate tiludronate-is activated resorption a prerequisite for the *in vivo* effect of PTH on formation in a remodeling system? Bone **16**: 603-610.

Dempster DW, Arlot MA, Meunier PJ (1983) Mean wall thickness and formation periods of trabecular bone packets in corticosteroid-induced osteoporosis. Calcif Tissue Int **35**: 410-417.

Dempster DW, Brown JP, Fahrleitner-Pammer A, Kendler D, Rizzo S, Valter I, Wagman RB, Yin X, Yue SV, Boivin G (2018) Effects of long-term denosumab on bone histomorphometry and mineralization in women with postmenopausal osteoporosis. J Clin Endocrinol Metab **103**: 2498-2509.

Dempster DW, Cosman F, Zhou H, Nieves JW, Bostrom M, Lindsay R (2016a) Effects of daily or cyclic teriparatide on bone formation in the iliac crest in women on no prior therapy and in women on alendronate. J Bone Miner Res **31**: 1518-1526.

Dempster DW, Zhou H, Recker RR, Brown JP, Bolognese MA, Recknor CP, Kendler DL, Lewiecki EM, Hanley DA, Rao SD, Miller PD, Woodson GC, Lindsay R, Binkley N, Alam J, Ruff VA, Gallagher ER, Taylor KA (2016b) A longitudinal study of skeletal histomorphometry at 6 and 24 months across four bone envelopes in postmenopausal women with osteoporosis receiving teriparatide or zoledronic acid in the SHOTZ trial. J Bone Miner Res **31**: 1429-1439.

Dovio A, Perazzolo L, Osella G, Ventura M, Termine A, Milano E, Bertolotto A, Angeli A (2004) Immediate fall of bone formation and transient increase of bone resorption in the course of high-dose, short-term glucocorticoid therapy in young patients with multiple sclerosis. J Clin Endocrinol Metab **89**: 4923-4928.

Drissi H, Lomri A, Lasmoles F, Holy X, Zerath E, Marie PJ (1999) Skeletal unloading induces biphasic changes in insulin-like growth factor-I mRNA levels and osteoblast activity. Exp Cell Res **251**: 275-284.

Ebeling PR, Erbas B, Hopper JL, Wark JD, Rubinfeld AR (1998) Bone mineral density and bone turnover in asthmatics treated with long- term inhaled or oral glucocorticoids. J Bone Miner Res **13**: 1283-1289.

Eriksen EF, Melsen F, Sod E, Barton I, Chines A (2002) Effects of long-term risedronate on bone quality and bone turnover in women with postmenopausal osteoporosis. Bone **31**: 620-625.

Eriksen EF, Hodgson SF, Eastell R, RIGGS BL, Cedel SL, O'Fallon WM (1990) Cancellous bone remodeling in type i (postmenopausal) osteoporosis: quantitative assessment of rates of formation, resorption, and bone loss at tissue and cellular levels. J Bone Miner Res **5**: 311-319.

Fan X, Roy E, Zhu L, Murphy TC, Ackert-Bicknell C, Hart CM, Rosen C, Nanes MS, Rubin J (2004) Nitric oxide regulates receptor activator of nuclear factor-κB ligand and osteoprotegerin expression in bone marrow stromal cells. Endocrinology **145**: 751-759.

Fan Y, Hanai J, Le PT, Dempster DW, Rosen CJ, Marrow B, Cell M, Fan Y, Hanai J, Le PT, Bi R, Maridas D, Demambro V, Figueroa CA (2017) Parathyroid hormone directs mesenchymal cell fate. Cell Metab **25**: 661-672.

Frost HM, Villanueva AR, Roth H, Stanisavljevic S (1961) Tetracycline bone labeling. J New Drugs **1**: 206-2016.

Frost HM (1987) Bone " mass " and the " mechanostat ": a proposal. Anat Rec **219**: 1-9.

Frost HM (1969) Tetracycline-based histological analysis of bone remodeling. Calcif Tissue Res **3**: 211-237.

Gabel L, Liphardt AM, Hulme PA, Heer M, Zwart SR, Sibonga JD, Smith SM, Boyd S (2021) Pre-flight exercise and bone metabolism predict unloading-induced bone loss due to spaceflight. Br J Sports Med **1**: 1-9.

Gaudio A, Pennisi P, Bratengeier C, Torrisi V, Lindner B, Mangiafico RA, Pulvirenti I, Hawa G, Tringali G, Fiore CE (2010) Increased Sclerostin serum levels associated with bone formation and resorption markers in patients with immobilization-induced bone loss. J Clin Endocrinol Metab **95**: 2248-2253.

Gauthier R, Follet H, Olivier C, Mitton D, Peyrin F (2019) 3D analysis of the osteonal and interstitial tissue in human radii cortical bone. Bone **127**: 526-536.

Genant HK, Engelke K, Bolognese MA, Mautalen C, Brown JP, Recknor C, Goemaere S, Fuerst T, Yang YC, Grauer A, Libanati C (2017) Effects of romosozumab compared with teriparatide on bone density and mass at the spine and hip in postmenopausal women with low bone mass. J Bone Miner Res **32**: 181-187.

Genetos DC, Geist DJ, Liu D, Donahue HJ, Duncan RL (2004) Fluid shear-induced ATP secretion mediates prostaglandin release in MC3T3-E1 osteoblasts. J Bone Miner Res **20**: 41-49.

Gerbaix M, Gnyubkin V, Farlay D, Olivier C, Ammann P, Courbon G, Laroche N, Genthial R, Follet H, Peyrin F, Shenkman B, Gauquelin-Koch G, Vico L (2017) One-month spaceflight compromises the bone microstructure, tissue-level mechanical properties, osteocyte survival and lacunae volume in mature mice skeletons. Sci Rep **7**: 2659. DOI: 10.1038/s41598-017-03014-2.

Giangregorio L, McCartney N (2006) Bone loss and muscle atrophy in spinal cord injury: epidemiology, fracture prediction, and rehabilitation strategies. J Spinal Cord Med **29**: 489-500.

Gifre L, Vidal J, Carrasco JL, Filella X, Ruiz-Gaspà S, Muxi A, Portell E, Monegal A, Guañabens N, Peris P (2015) Effect of recent spinal cord injury on WNT signaling antagonists (Sclerostin and Dkk-1) and their relationship with bone loss. A 12-month prospective study. J Bone Miner Res **30**: 1014-1021.

Godschalk MF, Downs RW (1988) Effect of short-term glucocorticoids on serum osteocalcin in healthy young men. J Bone Miner Res **3**: 113-115.

Hambli R (2014) Connecting mechanics and bone cell activities in the bone remodeling process: an integrated finite element modeling. Front Bioeng Biotechnol **2**: 1-12.

Hanley DA, Adachi JD, Bell A, Brown V (2012) Denosumab: mechanism of action and clinical outcomes. Int J Clin Pract **66**: 1139-1146.

Hansen S, Hauge EM, Beck Jensen JE, Brixen K (2013) Differing effects of PTH 1-34, PTH 1-84, and zoledronic acid on bone microarchitecture and estimated strength in postmenopausal women with osteoporosis: an 18-month open-labeled observational study using HR-pQCT. J Bone Miner Res **28**: 736-745.

Haris Á, Szabó A, Lányi É, Mucsi I, Polner K (2012) Acute and long-term effects of corticosteroid therapy on bone metabolism in patients with kidney diseases. Clin Nephrol **78**: 17-23.

van Harreveld PD, Lillich JD, Kawcak CE, Turner AS, Norrdin RW (2002) Effects of immobilization followed by remobilization on mineral density, histomorphometric features, and formation of the bones of the metacarpophalangeal joint in horses. Am J Vet Res **63**: 276-281.

Harris SE, Gluhak-Heinrich J, Harris MA, Yang W, Bonewald LF, Riha D, Rowe PSN, Robling AG, Turner CH, Feng JQ, McKee MD, Nicollela D (2007) DMP1 and MEPE expression are elevated in osteocytes after mechanical loading *in vivo*: theoretical role in controlling mineral quality in the perilacunar matrix. J Musculoskelet Neuronal Interact **7**: 1-7.

Harrison KD, Hiebert BD, Panahifar A, Andronowski JM, Ashique AM, King GA, Arnason T, Swekla KJ, Pivonka P, Cooper DML (2020a) Cortical bone porosity in rabbit models of osteoporosis. J Bone Miner Res **35**: 2211-2228.

Harrison KD, Cooper DML (2015) Modalities for visualization of cortical bone remodeling: the past, present, and future. Front Endocrinol (Lausanne) **6**: 1-9.

Hennig C, Thomas CDL, Clement JG, Cooper DML (2015) Does 3D orientation account for variation in osteon morphology assessed by 2D histology? J Anat **227**: 497-505.

Hernandez CJ, Gupta A, Keaveny TM (2006) A biomechanical analysis of the effects of resorption cavities on cancellous bone strength. J Bone Miner Res **21**: 1248-1255.

Hernández M V., Guañabens N, Alvarez L, Monegal A, Peris P, Riba J, Ercilla G, Martínez De Osaba MJ, Muñoz-Gómez J (2004) Immunocytochemical evidence on the effects of glucocorticoids on type I collagen synthesis in human osteoblastic cells. Calcif Tissue Int. **74**: 284-293.

Heřt J, Fiala P, Petrtýl M (1994) Osteon orientation of the diaphysis of the long bones in man. Bone **15**: 269-277.

Hirano T, Burr DB, Turner CH, Sato M, Cain RL, Hock JM (1999) Anabolic effects of Human biosynthetic parathhroid hormone fragment (1-34), LY333334, on remodeling and mechanical properties of cortical bone in rabbits. J Bone Miner Res **14**: 536-544.

Hock JM, Gera I (1992) Effects of continuous and intermittent administration and inhibition of resorption on the anabolic response of bone to parathyroid hormone. J Bone Miner Res **7**: 65-72.

Hofbauer LC, Gori F, Riggs BL, Lacey DL, Dunstan CR, Spelsberg TC, Khosla S (1999) Stimulation of osteoprotegerin ligand and inhibition of osteoprotegerin production by glucocorticoids in human osteoblastic lineage cells: potential paracrine mechanisms of glucocorticoid-induced osteoporosis. Endocrinology **140**: 4382-4389.

Hughes DE, Dai A, Tiffee JC, Li HH, Mundy GR, Boyce BF (1996) Estrogen promotes apoptosis of murine osteoclasts mediated by TGF-beta. Nat Med **2**: 1132-1136.

Iolascon G, Paoletta M, Liguori S, Curci C, Moretti A (2019) Neuromuscular diseases and bone. Front Endocrinol (Lausanne) **10**. DOI: 10.3389/fendo.2019.00794.

Ishijima M, Rittling SR, Yamashita T, Tsuji K, Kurosawa H, Nifuji A, Denhardt DT, Noda M (2001) Enhancement of osteoclastic bone resorption and suppression of osteoblastic bone formation in response to reduced mechanical stress do not occur in the absence of osteopontin. J Exp Med **193**: 399-404.

Jaworski ZF, Lok E (1972) The rate of osteoclastic bone erosion in Haversian remodeling sites of adult dog's rib. Calcif Tissue Res **10**: 103-112.

Jaworski ZF, Meunier P, Frost HM (1972) Observations on two types of resorption cavities in human lamellar cortical bone. Clin Orthop Relat Res **83**: 279-285.

Jensen PR, Andersen TL, Chavassieux P, Roux JP, Delaisse JM (2021) Bisphosphonates impair the onset of bone formation at remodeling sites. Bone **145**: 115850. DOI: 10.1016/j.bone.2021.115850.

Jensen PR, Andersen TL, Hauge EM, Bollerslev J, Delaissé JM (2015) A joined role of canopy and reversal cells in bone remodeling - lessons from glucocorticoid-induced osteoporosis. Bone **73**: 16-23.

Jia D, O'Brien CA, Stewart SA, Manolagas SC, Weinstein RS (2006) Glucocorticoids act directly on osteoclasts to increase their life span and reduce bone density. Endocrinology **147**: 5592-5599.

Jiang Y, Zhao JJ, Mitlak BH, Wang O, Genant HK, Eriksen EF (2003) Recombinant human parathyroid hormone (1-34) [teriparatide] improves both cortical and cancellous bone structure. J Bone Miner Res **18**: 1932-1941.

Jilka RL (1998) Cytokines, bone remodeling, and estrogen deficiency: a 1998 update. Bone **23**: 75-81.

Jilka RL, Hangoc G, Girasole G, Passeri G, Williams DC, Abrams JS, Boyce B, Broxmeyer H, Manolagas SC (1992) Increased osteoclast development after estrogen loss: mediation by interleukin-6. Science **257**: 88-91.

Jilka RL, Weinstein RS, Bellido T, Roberson P, Parfitt AM, Manolagas SC (1999) Increased bone formation by prevention of osteoblast apoptosis with parathyroid hormone. J Clin Invest **104**: 439-446.

Johnson L (1964) Morphological analysis in pathology. In: Bone Biodyn. Editor: HM Frost. pp: 543-654. Boston, Little, Brown, and Company.

Jorgenson BL, Buie HR, McErlain DD, Sandino C, Boyd SK (2015) A comparison of methods for *in vivo* assessment of cortical porosity in the human appendicular skeleton. Bone **73**: 167-175.

Jowsey J (1966) Studies of Haversian systems in man and some animals. J Anat **100**: 857-85764.

Kameo Y, Miya Y, Hayashi M, Nakashima T, Adachi T (2020) *In silico* experiments of bone remodeling explore metabolic diseases and their drug treatment. Sci Adv **6**: 1-11.

Kazakia GJ, Tjong W, Nirody JA, Burghardt AJ, Carballido-Gamio J, Patsch JM, Link T, Feeley BT, Benjamin Ma C (2014) The influence of disuse on bone microstructure and mechanics assessed by HR-pQCT. Bone **63**: 132-140.

Kenkre JS, Bassett JHD (2018) The bone remodelling cycle. Ann Clin Biochem **55**: 308-327.

Kim HJ, Zhao H, Kitaura H, Bhattacharyya S, Brewer JA, Muglia LJ, Ross FP, Teitelbaum SL (2006) Glucocorticoids suppress bone formation *via* the osteoclast. J Clin Invest **116**: 2152-2160.

Kimmel DB, Recker RR, Gallagher JC, Vaswani AS, Aloia JF (1990) A comparison of iliac bone histomorphometric data in post-menopausal osteoporotic and normal subjects. Bone Miner **11**: 217-235.

Kondo H, Nifuji A, Takeda S, Ezura Y, Rittling SR, Denhardt DT, Nakashima K, Karsenty G, Noda M (2005) Unloading induces osteoblastic cell suppression and osteoclastic cell activation to lead to bone loss *via* sympathetic nervous system. J Biol Chem **280**: 30192-30200.

Kostenuik PJ, Nguyen HQ, Mccabe J, Warmington KS, Kurahara C, Sun N, Chen C, Li L, Cattley RC, Van G, Scully S, Elliott R, Grisanti M, Morony S, Tan HL, Asuncion F, Li X, Ominsky MS, Stolina M, Dwyer D, Dougall WC, Hawkins N, Boyle WJ, Simonet WS, Sullivan JK (2009) Denosumab, a fully human monoclonal antibody to RANKL, inhibits bone resorption and increases BMD in knock-in mice that express chimeric (murine/human) RANKL. J Bone Miner Res **24**: 182-195.

Kostenuik PJ, Smith SY, Samadfam R, Jolette J, Zhou L, Ominsky MS (2015) Effects of denosumab, slendronate, or denosumab following alendronate on bone turnover, calcium homeostasis, bone mass and bone strength in ovariectomized cynomolgus monkeys. J Bone Miner Res **30**: 657-669.

Krum SA, Miranda-Carboni GA, Hauschka P V., Carroll JS, Lane TF, Freedman LP, Brown M (2008) Estrogen protects bone by inducing Fas ligand in osteoblasts to regulate osteoclast survival. EMBO J **27**: 535-545.

Lacey DL, Timms E, Tan HL, Kelley MJ, Dunstan CR, Burgess T, Elliott R, Colombero A, Elliott G, Scully S, Hsu H, Sullivan J, Hawkins N, Davy E, Capparelli C, Eli A, Qian YX, Kaufman S, Sarosi I, Shalhoub V, Senaldi G, Guo J, Delaney J, Boyle WJ (1998) Osteoprotegerin ligand is a cytokine that regulates osteoclast differentiation and activation. Cell **93**: 165-176.

Lambers FM, Kuhn G, Schulte FA, Koch K, Müller R (2012) Longitudinal assessment of *in vivo* bone dynamics in a mouse tail model of postmenopausal osteoporosis. Calcif Tissue Int **90**: 108-119.

Lambers FM, Kuhn G, Weigt C, Koch KM, Schulte FA, Müller R (2015) Bone adaptation to cyclic loading in murine caudal vertebrae is maintained with age and directly correlated to the local micromechanical environment. J Biomech **48**: 1179-1187.

Langdahl BL, Libanati C, Crittenden DB, Bolognese MA, Brown JP, Daizadeh NS, Dokoupilova E, Engelke K, Finkelstein JS, Genant HK, Goemaere S, Hyldstrup L, Jodar-Gimeno E, Keaveny TM, Kendler D, Lakatos P, Maddox J, Malouf J, Massari FE, Molina JF, Ulla MR, Grauer A (2017) Romosozumab (sclerostin monoclonal antibody) *versus* teriparatide in postmenopausal women with osteoporosis transitioning from oral bisphosphonate therapy: a randomised, open-label, phase 3 trial. Lancet **390**: 1585-1594.

Lassen NE, Andersen, Thomas Levin Pløen GG, Søe K, Hauge, Ellen Margrethe Harving S, Eschen GET, Delaisse J-M, 1Clinical (2017) Coupling of bone resorption and formation in real time: new knowledge gained from human haversian BMUs. J Bone Miner Res **32**: 1395-1405.

Li CY, Price C, Delisser K, Nasser P, Laudier D, Clement M, Jepsen KJ, Schaffler MB (2004) Long-term disuse osteoporosis seems less sensitive to bisphosphonate treatment than other osteoporosis. J Bone Miner Res **20**: 117-124.

Li J, Sarosi I, Cattley RC, Pretorius J, Asuncion F, Grisanti M, Morony S, Adamu S, Geng Z, Qiu W, Kostenuik P, Lacey DL, Simonet WS, Bolon B, Qian X, Shalhoub V, Ominsky MS, Zhu Ke H, Li X, Richards WG (2006) Dkk1-mediated inhibition of Wnt signaling in bone results in osteopenia. Bone **39**: 754-766.

Li XJ, Jee WSS (1991) Adaptation of diaphyseal structure to aging and decreased mechanical loading in the adult rat: a densitometric and histomorphometric study. Anat Rec **229**: 291-297.

Li XJ, Jee WSS, Chow S-Y, Woodbury D (1990) Adaptation of cancellous bone to aging and immobilization in the rat: a single photon absorptiometry and histomorphometry study. Anat Rec **227**: 418-426.

Li X, Ominsky MS, Warmington KS, Morony S, Gong J, Cao J, Gao Y, Shalhoub V, Tipton B, Haldankar R, Chen Q, Winters A, Boone T, Geng Z, Niu QT, Ke HZ, Kostenuik PJ, Simonet WS, Lacey DL, Paszty C (2009) Sclerostin antibody treatment increases bone formation, bone mass, and bone strength in a rat model of postmenopausal osteoporosis. J Bone Miner Res **24**: 578-588.

Li Z, Kuhn G, von Salis-Soglio M, Cooke SJ, Schirmer M, Müller R, Ruffoni D (2015) *In vivo* monitoring of bone architecture and remodeling after implant insertion: the different responses of cortical and trabecular bone. Bone **81**: 468-477.

Lin C, Jiang X, Dai Z, Guo X, Weng T, Wang J, Li Y, Feng G, Gao X, He L (2009) Sclerostin mediates bone response to mechanical unloading through antagonizing Wnt/β-catenin signaling. J Bone Miner Res **24**: 1651-1661.

Lindsay R, Zhou H, Cosman F, Nieves J, Dempster DW, Hodsman AB (2007) Effects of a one-month treatment with PTH(1-34) on bone formation on cancellous, endocortical, and periosteal surfaces of the human ilium. J Bone Miner Res **22**: 495-502.

Liu L, Li H, Cui Y, Li R, Meng F, Ye Z, Zhang X (2017) Calcium channel opening rather than the release of ATP causes the apoptosis of osteoblasts induced by overloaded mechanical stimulation. Cell Physiol Biochem **42**: 441-454.

Locklin RM, Khosla S, Turner RT, Riggs BL (2003) Mediators of the biphasic responses of bone to intermittent and continuously administered parathyroid hormone. J Cell Biochem **89**: 180-190.

Loundagin LL, Pohl AJ, Edwards WB (2020) Stressed volume estimated by finite element analysis predicts the fatigue life of human cortical bone: the role of vascular canals as stress concentrators. Bone: **143**: 115647. DOI: 10.1016/j.bone.2020.115647.

Ma YL, Zeng QQ, Chiang AY, Burr D, Li J, Dobnig H, Fahrleitner-Pammer A, Michalská D, Marin F, Pavo I, Stepan JJ (2014) Effects of teriparatide on cortical histomorphometric variables in postmenopausal women with or without prior alendronate treatment. Bone **59**: 139-147.

MacDonald HM, Nishiyama KK, Hanley DA, Boyd SK (2011) Changes in trabecular and cortical bone microarchitecture at peripheral sites associated with 18 months of teriparatide therapy in postmenopausal women with osteoporosis. Osteoporos Int **22**: 357-362.

Maggiano IS, Maggiano CM, Clement JG, Thomas CDL, Carter Y, Cooper DML (2016) Three-dimensional reconstruction of Haversian systems in human cortical bone using synchrotron radiation-based μCT: morphology and quantification of branching and transverse connections across age. J Anat **228**: 719-732.

Maïmoun L, Couret I, Mariano-Goulart D, Dupuy AM, Micallef JP, Peruchon E, Ohanna F, Cristol JP, Rossi M, Leroux JL (2005) Changes in osteoprotegerin/RANKL system, bone mineral density, and bone biochemicals markers in patients with recent spinal cord injury. Calcif Tissue Int **76**: 404-411.

Mann V, Huber C, Kogianni G, Jones D, Noble B (2006) The influence of mechanical stimulation on osteocyte apoptosis and bone viability in human trabecular bone. J Musculoskelet Neuronal Interact. **6**: 408-417.

Martin RB (1991) On the significance of remodeling space and activation rate changes in bone remodeling. Bone **12**: 391-400.

Martínez-Reina J, García-Aznar JM, Domínguez J, Doblaré M (2009) A bone remodelling model including the directional activity of BMUs. Biomech Model Mechanobiol **8**: 111-127.

Martínez-Reina J, Reina I, Domínguez J, García-Aznar JM (2014) A bone remodelling model including the effect of damage on the steering of BMUs. J Mech Behav Biomed Mater **32**: 99-112.

McCladen R, Mgeough J, Barker M (1993) Age-related changes in the tensile properties of cortical bone. J Bone Jt Surg **75**: 1193-1205.

McClung MR, Grauer A, Boonen S, Bolognese MA, Brown JP, Diez-Perez A, Langdahl BL, Reginster J-Y, Zanchetta JR, Wasserman SM, Katz L, Maddox J, Yang Y-C, Libanati C, Bone HG (2014) Romosozumab in postmenopausal women with low bone mineral density. N Engl J Med **370**: 412-20.

Mourad C, Laperre K, Halut M, Galant C, Van Cauter M, Vande Berg BC (2018) Fused micro-computed tomography (μCT) and histological images of bone specimens. Diagn Interv Imaging **99**: 501-505.

Mullender MG, Huiskes R (1995) Proposal for the regulatory mechanism of Wolff's law. J Orthop Res **13**: 503-512.

Nabavi N, Khandani A, Camirand A, Harrison RE (2011) Effects of microgravity on osteoclast bone resorption and osteoblast cytoskeletal organization and adhesion. Bone **49**: 965-974.

Nakamura T, Imai Y, Matsumoto T, Sato S, Takeuchi K, Igarashi K, Harada Y, Azuma Y, Krust A, Yamamoto Y, Nishina H, Takeda S, Takayanagi H, Metzger D, Kanno J, Takaoka K, Martin TJ, Chambon P, Kato S (2007) Estrogen prevents bone loss *via* estrogen receptor α and induction of FAS ligand in osteoclasts. Cell **130**: 811-823.

Nepal AK, van Essen HW, van der Veen AJ, van Wieringen WN, Stavenuiter AWD, Cayami FK, Pals G, Micha D, Vanderschueren D, Lips P, Bravenboer N (2021) Mechanical stress regulates bone regulatory gene expression independent of estrogen and vitamin D deficiency in rats. J Orthop Res **39**: 42-52.

Nicolella DP, Moravits DE, Gale AM, Bonewald LF, Lankford J (2006) Osteocyte lacunae tissue strain in cortical bone. J Biomech **39**: 1735-1743.

van Oers RFM, Ruimerman R, Tanck E, Hilbers PAJ, Huiskes R (2008a) A unified theory for osteonal and hemi-osteonal remodeling. Bone **42**: 250-259.

van Oers RFM, Ruimerman R, van Rietbergen B, Hilbers PAJ, Huiskes R (2008b) Relating osteon diameter to strain. Bone **43**: 476-482.

Ohnaka K, Taniguchi H, Kawate H, Nawata H, Takayanagi R (2004) Glucocorticoid enhances the expression of dickkopf-1 in human osteoblasts: novel mechanism of glucocorticoid-induced osteoporosis. Biochem Biophys Res Commun **318**: 259-264.

Ominsky MS, Boyd SK, Varela A, Jolette J, Felx M, Doyle N, Mellal N, Smith SY, Locher K, Buntich S, Pyrah I, Boyce RW (2017) Romosozumab improves bone mass and strength while maintaining bone quality in ovariectomized cynomolgus monkeys. J Bone Miner Res **32**: 788-801.

Pacifici R, Brown C, Puscheck E, Friedrich E, Slatopolsky E, Maggio D, Mccracken R, Avioli L V. (1991) Effect of surgical menopause and estrogen replacement on cytokine release from human blood mononuclear cells. Proc Natl Acad Sci U S A **88**: 5134-5138.

Padhi D, Jang G, Stouch B, Fang L, Posvar E (2011) Single-dose, placebo-controlled, randomized study of AMG 785, a sclerostin monoclonal antibody. J Bone Miner Res **26**: 19-26.

Panahifar A, Swanston TM, Jake Pushie M, Belev G, Chapman D, Weber L, Cooper DML (2016) Three-dimensional labeling of newly formed bone using synchrotron radiation barium K-edge subtraction imaging. Phys Med Biol **61**: 5077-5088.

Parfitt AM (1982) The coupling of bone formation to bone resorption: a critical analysis of the concept and of its relevance to the pathogenesis of osteoporosis. Metab Bone Dis Relat Res **4**: 1-6.

Parfitt AM (1994) Osteonal and hemi-osteonal remodeling: the spatial and temporal framework for signal traffic in adult human bone. J Cell Biochem **55**: 273-286.

Parfitt AM, Villanueva AR, Foldes J, Rao DS (1995) Relations between histologic indices of bone formation: implications for the pathogenesis of spinal osteoporosis. J Bone Miner Res **10**: 466-473.

Particelli F, Mecozzi L, Beraudi A, Montesi M, Baruffaldi F, Viceconti M (2012) A comparison between μCT and histology for the evaluation of cortical bone: effect of polymethylmethacrylate embedding on structural parameters. J Microsc **245**: 302-310.

Patterson-Buckendahl P, Arnaud SB, Mechanic GL, Martin RB, Grindeland RE, Cann CE (1987) Fragility and composition of growing rat bone after one week in spaceflight. Am J Physiol **252**: 240-246.

Pazzaglia UE, Zarattini G, Giacomini D, Rodella L, Menti AM, Feltrin G (2009) Morphometric analysis of the canal system of cortical bone : an experimental study in the rabbit femur carried out with standard histology and μCT. Jounral Vet Med **39**: 17-26.

Pereira RC, Delany AM, Canalis E (2002) Effects of cortisol and bone morphogenetic protein-2 on stromal cell differentiation: correlation with CCAAT-enhancer binding protein expression. Bone **30**: 685-691.

Peretz A, Praet JP, Bosson D, Rozenberg S, Bourdoux P (1989) Serum osteocalcin in the assessment of corticosteroid induced osteoporosis. Effect of long and short term corticosteroid treatment. J Rheumatol **16**: 363-367.

Petrtýl M, Heřt J, Fiala P (1996) Spatial organization of the haversian bone in man. J Biomech **29**: 161-169.

Pisani P, Renna MD, Conversano F, Casciaro E, Di Paola M, Quarta E, Muratore M, Casciaro S (2016) Major osteoporotic fragility fractures: risk factor updates and societal impact. World J Orthop **7**: 171-181.

Pivonka P, Komarova S V. (2010) Mathematical modeling in bone biology: from intracellular signaling to tissue mechanics. Bone **47**: 181-189.

Plotkin LI, Mathov I, Aguirre JI, Parfitt AM, Manolagas SC, Bellido T (2005) Mechanical stimulation prevents osteocyte apoptosis: requirement of integrins, Src kinases, and ERKs. Am J Physiol **289**: 633-643.

Pratt IV, Belev G, Zhu N, Chapman LD, Cooper DML (2015) *In vivo* imaging of rat cortical bone porosity by synchrotron phase contrast micro computed tomography. Phys Med Biol **60**: 211-232.

Prummel MF, Wiersinga WM, Lips P, Sanders GTB, Sauerwein HP (1991) The course of biochemical parameters of bone turnover during treatment with corticosteroids. J Clin Endocrinol Metab **72**: 382-386.

Ralston SH, Ho L-P, Helfrich MH, Grabowski PS, Johnston PW, Benjamin N (1995) Nitric oxide: a cytokine-induced regulator of bone resorption. J Bone Miner Res **10**: 1040-1049.

Ramchand SK, Seeman E (2018) The influence of cortical porosity on the strength of bone during growth and advancing age. Curr Osteoporos Rep **16**: 561-572.

Recker RR, Delmas PD, Halse J, Reid IR, Boonen S, Garcia-Hernandez PA, Supronik J, Lewiecki EM, Ochoa L, Miller P, Hu H, Mesenbrink P, Hartl F, Gasser J, Eriksen EF (2008) Effects of intravenous zoledronic acid once yearly on bone remodeling and bone structure. J Bone Miner Res **23**: 6-16.

Reid IR, Miller PD, Brown JP, Kendler DL, Fahrleitner-pammer A, Valter I, Maasalu K, Bolognese MA, Woodson G, Bone H, Ding B, Wagman RB, Martin JS, Ominsky MS (2010) Effects of denosumab on bone histomorphometry: the FREEDOM and STAND studies. J Bone Miner Res **25**: 2256-2265.

Reszka AA, Rodan GA (2003) Bisphosphonate mechanism of action. Curr Rheumatol Rep **5**: 65-74.

Roberts WE, Roberts JA, Epker BN, Burr DB, Hartsfield JK (2006) Remodeling of mineralized tissues, part I: the frost legacy. Semin Orthod **12**: 216-237.

Roberts WE, Smith RK, Zilberman Y, Mozsary PG, Smith RS (1984) Osseous adaptation to continuous loading of rigid endosseous implants. Am J Orthod **86**: 95-111.

Robling AG, Stout SD (1999) Morphology of the drifting osteon. Cells Tissues Organs **164**: 192-204.

Rolvien T, Amling M (2021) Disuse osteoporosis: clinical and mechanistic insights. Calcif Tissue Int **110**: 592-604.

Rolvien T, Milovanovic P, Schmidt FN, von Kroge S, Wölfel EM, Krause M, Wulff B, Püschel K, Ritchie RO, Amling M, Busse B (2020) Long-term immobilization in elderly females causes a specific pattern of cortical bone and osteocyte deterioration different from postmenopausal osteoporosis. J Bone Miner Res **35**: 1343-1351.

Rubin MR, Dempster DW, Zhou H, Shane E, Nickolas T, Sliney J, Silverberg SJ, Bilezikian JP (2008) Dynamic and structural properties of the skeleton in hypoparathyroidism. J Bone Miner Res **23**: 2018-2024.

Rueckert D, Schnabel JA (2011) Medical image registration. In: Biomedical Image Processing. Editor: TM Deserno. pp: 131-155. Springer Berlin Heidelberg.

Ryser MD, Nigam N, Komarova S V (2009) Mathematical modeling of spatio-temporal dynamics of a single bone multicellular Unit **24**: 860-870.

Saika M, Matsumoto T (2001) 17beta-estradiol stimulates expression of osteoprotegerin by a mouse stromal cell line, ST-2, *via* estrogen receptor-alpha. Endocrinology **142**: 2205-2212.

Saito M, Marumo K, Ushiku C, Kato S, Sakai S, Hayakawa N, Mihara M, Shiraishi A (2011) Effects of alfacalcidol on mechanical properties and collagen cross-links of the femoral diaphysis in glucocorticoid-treated rats. Calcif Tissue Int **88**: 314-324.

Santos A, Bakker AD, Klein-Nulend J (2009) The role of osteocytes in bone mechanotransduction. Osteoporos Int **20**: 1027-1031.

Sasaki N, Kusano E, Ando Y, Nemoto J, Iimura O, Ito C, Takeda S, Yano K, Tsuda E, Asano Y (2002) Changes in osteoprotegerin and markers of bone metabolism during glucocorticoid treatment in patients with chronic glomerulonephritis. Bone **30**: 853-858.

Sato M, Westmore M, Ma YL, Schmidt A, Zeng QQ, Glass E V., Vahle J, Brommage R, Jerome CP, Turner CH (2004) Teriparatide [PTH(1-34)] strengthens the proximal femur of ovariectomized nonhuman primates despite increasing porosity. J Bone Miner Res **19**: 623-629.

Schenk R, Willenegger H (1964) Zur Histologie der primairen Knochenheilung. Langenbecks Arch für Klin Chir **308**: 440-452.

Schock CC, Noyes FR, Crouch MM, Mathews CHE (1975) The effects of immobility on long bone remodelling in the rhesus monkey. Henry Ford Hosp Med J **23**: 107-116.

Schorlemmer S, Ignatius A, Claes L, Augat P (2005) Inhibition of cortical and cancellous bone formation in glucocorticoid-treated OVX sheep. Bone **37**: 491-496.

Schulte FA, Lambers FM, Kuhn G, Muller R (2011a) *In vivo* micro-computed tomography allows direct three-dimensional quantification of both bone formation and bone resorption parameters using time-lapsed imaging. Bone **48**: 433-442.

Schulte FA, Lambers FM, Webster DJ, Kuhn G, Muller R (2011b) *In vivo* validation of a computational bone adaptation model using open-loop control and time-lapsed micro-computed tomography. Bone **49**: 1166-1172.

Schulte FA, Ruffoni D, Lambers FM, Christen D, Webster DJ, Kuhn G, Müller R (2013a) Local mechanical stimuli regulate bone formation and resorption in mice at the tissue level. PLoS One **8**. DOI: 10.1371/journal.pone.0062172.

Schulte FA, Zwahlen A, Lambers FM, Kuhn G, Ruffoni D, Betts D, Webster DJ, Müller R (2013b) Strain-adaptive *in silico* modeling of bone adaptation — a computer simulation validated by *in vivo* micro-computed tomography data. Bone **52**: 485-492.

Seeman E, Delmas PD, Hanley DA, Sellmeyer D, Cheung AM, Shane E, Kearns A, Thomas T, Boyd SK, Boutroy S, Bogado C, Majumdar S, Fan M, Libanati C, Zanchetta J (2010) Microarchitectural deterioration of cortical and trabecular bone: differing effects of denosumab and alendronate. J Bone Miner Res **25**: 1886-1894.

Shevde NK, Bendixen AC, Dienger KM, Pike JW (2000) Estrogens suppress RANK ligand-induced osteoclast differentiation via a stromal cell independent mechanism involving c-Jun repression. Proc Natl Acad Sci U S A **97**: 7829-7834.

Sivagurunathan S, Muir MM, Brennan TC, Seale JP, Mason RS (2005) Influence of glucocorticoids on human osteoclast generation and activity. J Bone Miner Res **20**: 390-398.

Slyfield CR, Tkachenko EV, Wilson DL, Hernandez CJ (2012) Three-dimensional dynamic bone histomorphometry. J Bone Miner Res **27**: 486-495.

Smit TH, Burger EH, Huyghe JM (2002) A case for strain-induced fluid flow as a regulator of BMU-coupling and osteonal alignment. J Bone Miner Res **17**: 2021-2029.

Smit TH, Burger EH (2000) Is BMU-coupling a strain-regulated phenomenon? A finite element analysis. J Bone Miner Res **15**: 301-307.

Smith DW, Gardiner BS, Dunstan C (2012) Bone balance within a cortical BMU: local controls of bone resorption and formation. PLoS One **7**: 17-21.

Soltan N, Kawalilak CE, Cooper DM, Kontulainen SA, Johnston JD (2019) Cortical porosity assessment in the distal radius: a comparison of HR-pQCT measures with synchrotron-radiation μCT-based measures. Bone **120**: 439-445.

Sozen T, Ozisik L, Calik Basaran N (2017) An overview and management of osteoporosis. Eur J Rheumatol **4**: 46-56.

Spatz JM, Fields EE, Yu EW, Divieti Pajevic P, Bouxsein ML, Sibonga JD, Zwart SR, Smith SM (2012) Serum sclerostin increases in healthy adult men during bed rest. J Clin Endocrinol Metab **97**: 1736-1740.

Van Staa TP, Leufkens HGM, Cooper C (2002) The epidemiology of corticosteroid-induced osteoporosis: a meta-analysis. Osteoporos Int **13**: 777-787.

Stavnichuk M, Mikolajewicz N, Corlett T, Morris M, Komarova SV (2020) A systematic review and meta-analysis of bone loss in space travelers. NPJ Microgravity **6**. 13. DOI: 10.1038/s41526-020-0103-2.

Stout SD, Brunsden BS, Hildebolt CF, Commean PK, Smith KE, Tappen NC (1999) Computer-assisted 3D reconstruction of serial sections of cortical bone to determine the 3D structure of osteons. Calcif Tissue Int **65**: 280-284.

Takahashi H, Ota M, Norimatsu H (1971) A tetracyline-based study of a linear rate of bone-matrix mmineralization in canine bones. Acta Med Biol (Niigata) **18**: 269-274.

Tamma R, Colaianni G, Camerino C, Di Benedetto A, Greco G, Strippoli M, Vergari R, Grano A, Mancini L, Mori G, Colucci S, Grano M, Zallone A (2009) Microgravity during spaceflight directly affects *in vitro* osteoclastogenesis and bone resorption. FASEB J **23**: 2549-2554.

Tang Y, Wu X, Lei W, Pang L, Wan C, Shi Z, Zhao L, Nagy TR, Peng X, Hu J, Feng X, Van Hul W, Wan M, Cao X (2009) TGF-B1-induced migration of bone mesenchymal stem cells couples bone resorption with formation. Nat Med **15**: 757-765.

Tappen NC (1977) Three-dimensional studies of resorption spaces and developing osteons. Am J Anat **149**: 301-332.

Tsubota K ichi, Suzuki Y, Yamada T, Hojo M, Makinouchi A, Adachi T (2009) Computer simulation of trabecular remodeling in human proximal femur using large-scale voxel FE models: approach to understanding Wolff's law. J. Biomech. **42**: 1088-1094.

Turner RT, Bell NH (1986) The effects of immobilization on bone histomorphometry in rats. J Bone Miner Res **1**: 399-407.

Vandenbroucke A, Luyten FP, Flamaing J, Gielen E (2017) Pharmacological treatment of osteoporosis in the oldest old. Clin Interv Aging **12**: 1065-1077.

Vedi S, Elkin SL, Compston JE (2005) A histomorphometric study of cortical bone of the iliac crest in patients treated with glucocorticoids. Calcif Tissue Int **77**: 79-83.

Vu TDT, Wang XF, Wang Q, Cusano NE, Irani D, Silva BC, Ghasem-Zadeh A, Udesky J, Romano ME, Zebaze R, Jerums G, Boutroy S, Bilezikian JP, Seeman E (2013) New insights into the effects of primary hyperparathyroidism on the cortical and trabecular compartments of bone. Bone **55**: 57-63.

Waarsing JH, Day JS, Van Der Linden JC, Ederveen AG, Spanjers C, De Clerck N, Sasov A, Verhaar

JAN, Weinans H (2004) Detecting and tracking local changes in the tibiae of individual rats: a novel method to analyse longitudinal *in vivo* µCT data. Bone **34**: 163-169.

Wachter NJ, Krischak GD, Mentzel M, Sarkar MR, Ebinger T, Kinzl L, Claes L, Augat P (2002) Correlation of bone mineral density with strength and microstructural parameters of cortical bone *in vitro*. Bone **31**: 90-95.

Wang L, Liu S, Zhao Y, Liu D, Liu Y, Chen C, Karray S, Shi S, Jin Y (2015) Osteoblast-induced osteoclast apoptosis by fas ligand/FAS pathway is required for maintenance of bone mass. Cell Death Differ **22**: 1654-1664.

Weinreb M, Rodan GA, Thompson DD (1989) Osteopenia in the immobilized rat hind limb is associated with increased bone resorption and decreased bone formation. Bone **10**: 187-194.

Weinstein RS, Jilka RL, Michael Parfitt A, Manolagas SC (1998) Inhibition of osteoblastogenesis and promotion of apoptosis of osteoblasts end osteocytes by glucocorticoids potential mechanisms of their deleterious effects on bone. J Clin Invest **102**: 274-282.

Weitzmann MN, Pacifici R (2006) Estrogen deficiency and bone loss: an inflammatory tale. J Clin Invest **116**: 1186-1194.

Whittier X, Saag KG (2016) Glucocorticoid-induced osteoporosis. Rheum Dis Clin North Am **42**: 177-189.

Wijenayaka AR, Kogawa M, Lim HP, Bonewald LF, Findlay DM, Atkins GJ (2011) Sclerostin stimulates osteocyte support of osteoclast activity by a RANKL-dependent pathway **6**: e25900. DOI: 10.1371/journal.pone.0025900.

Wu X, Pang L, Lei W, Lu W, Li J, Li Z, Frassica FJ, Chen X, Wan M, Cao X (2010) Inhibition of sca-1-positive skeletal stem cell recruitment by alendronate blunts the anabolic effects of parathyroid hormone on bone remodeling. Cell Stem Cell **7**: 571-580.

Xi L, Song Y, Wu W, Qu Z, Wen J, Liao B, Tao R, Ge J, Fang D (2020) Investigation of bone matrix composition, architecture and mechanical properties reflect structure-function relationship of cortical bone in glucocorticoid induced osteoporosis. Bone **136**: 115334. DOI: 10.1016/j.bone.2020.115334.

Xiong J, Onal M, Jilka RL, Weinstein RS, Manolagas SC, O'Brien CA (2011) Matrix-embedded cells control osteoclast formation. Nat Med **17**: 1235-1241.

Xu H, Wu J, Weng Y, Zhang J, Shang P (2012) Two-dimensional clinorotation influences cellular morphology, cytoskeleton and secretion of MLO-Y4 osteocyte-like cells. Biologia (Bratisl) **67**: 255-262.

Yamamoto T, Hasegawa T, Sasaki M, Hongo H, Tsuboi K, Shimizu T, Ota M, Haraguchi M, Takahata M, Oda K, De Freitas PHL, Takakura A, Takao-Kawabata R, Isogai Y, Amizuka N (2016) Frequency of teriparatide administration affects the histological pattern of bone formation in young adult male mice. Endocrinology **157**: 2604-2620.

Yamane H, Takakura A, Shimadzu Y, Kodama T, Lee JW, Isogai Y, Ishizuya T, Takao-Kawabata R, Iimura T (2017) Acute development of cortical porosity and endosteal naïve bone formation from the daily but not weekly short-term administration of PTH in rabbit. PLoS One **12**: 1-26.

Yang W, Lu Y, Kalajzic I, Guo D, Harris MA, Gluhak-Heinrich J, Kotha S, Bonewald LF, Feng JQ, Rowe DW, Turner CH, Robling AG, Harris SE (2005) Dentin matrix protein 1 gene cis-regulation: Use in osteocytes to characterize local responses to mechanical loading *in vitro* and *in vivo*. J Biol Chem **280**: 20680-20690.

Yao W, Cheng Z, Pham A, Busse C, Zimmermann EA, Ritchie RO, Lane NE (2008) Glucocorticoid-induced bone loss in mice can be reversed by the actions of parathyroid hormone and risedronate on different pathways for bone formation and mineralization. Arthritis Rheum **58**: 3485-3497.

Young DR, Niklowitz WJ, Brown RJ, Jee WSS (1986) Immobilization-associated osteoporosis in primates. Bone **7**: 109-117.

Zebaze RM, Ghasem-Zadeh A, Bohte A, Iuliano-Burns S, Mirams M, Price RI, Mackie EJ, Seeman E (2010) Intracortical remodelling and porosity in the distal radius and post-mortem femurs of women: a cross-sectional study. Lancet **375**: 1729-1736.

Zerath E, Novikov V, Leblanc A, Bakulin A, Oganov V, Grynpas M (1996) Effects of spaceflight on bone mineralization in the rhesus monkey. J Appl Physiol **81**: 194-200.

Zerwekh JE, Ruml LA, Gottschalk F, Pak CYC (1998) The effects of twelve weeks of bed rest on bone histology, biochemical markers of bone turnover, and calcium homeostasis in eleven normal subjects. J Bone Miner Res **13**: 1594-1601.

Zimmermann EA, Schaible E, Gludovatz B, Schmidt FN, Riedel C, Krause M, Vettorazzi E, Acevedo C, Hahn M, Puschel K, Tang S, Amling M, Ritchie RO, Busse B (2016) Intrinsic mechanical behavior of femoral cortical bone in young, osteoporotic and bisphosphonate-treated individuals in low-and high energy fracture conditions. Sci Rep **6**: 1-12.

Web References

1. https://health-products.canada.ca/noc-ac/info.do?lang=en&no=22291 [19-04-2022]

2. https://www.fda.gov/news-events/press-announcements/fda-approves-new-treatment-osteoporosis-postmenopausal-women-high-risk-fracture [19-04-2022]

Discussion with Reviewer

Reviewer: What is the role of the local mechanical environment on BMU activity and how can this be isolated from other systemic factors?

Authors: The local mechanical environment is thought to play a role in nearly all aspects of bone remodelling, potentially determining the initiation site of a BMU, its trajectory, the volume of bone resorbed and formed as well as the coupling of the resorption and formation phases. Direct *in vivo* evidence confirms that the site of remodelling and the amount of bone resorbed and formed is directly related to the local mechanical environment (*e.g.* strain energy density); however, this has only been demonstrated in trabecular and endocortical bone and remains unknown for intracortical bone. The link between the mechanical environment and BMU trajectories in cortical bone was originally inferred from observational studies that noted the alignment of Haversian systems with the principal loading direction in long bones. While computational models have since substantiated this hypothesis, explicit manipulation of the mechanical loading environment and its effects on BMU trajectory have not been studied in depth. Similarly, a few different mechanisms by which the local mechanical environment regulates the coupling of bone resorption and formation have been proposed but experimental evidence is lacking. The reduced bone formation observed after unloading supports the notion that mechanical stimuli affect formative activity but does not demonstrate complete uncoupling due to changes in the mechanical environment.

The local mechanical environment may control these aspects of BMU activity through a cellular response, primarily through mechanical stimulation of osteocytes and subsequent release of various biochemical messengers. The mechanotransducive role of osteocytes tightly regulates local bone resorption and formation through the RANKL/OPG and WNT signalling pathways; however, systematic factors such as hormones and nutrition also affect bone turnover. Some of these systematic factors also act directly on the RANKL/OPG or WNT signalling pathways and it may be difficult, if not impossible, to completely isolate their effects on BMU activity from that of the mechanical environment. Knockout or transgenic animal models are an appealing option to remove the influence of systematic factors but are generally limited to small animals and pre-clinical research. Even if systematic factors could be perfectly controlled, it should not be ruled out that the influence of the mechanical environment on remodelling is likely co-dependent and modulated by systematic factors. Therefore, completely removing them would alter the observed response to mechanical loading. An alternative approach may be to not isolate, but account for, systematic factors. For example, if one could quantify the mechanical sensitivity in an osteoporosis and control model, then it would be possible to determine the extent to which systematic factors known to be different between conditions (*e.g.* oestrogen) contribute to the remodelling response *versus* the response due to the mechanical stimuli.

Editor's note: The Scientific Editor responsible for this paper was Stephen Ferguson.